



# Room temperature line lists for CO<sub>2</sub> symmetric isotopologues with *ab initio* computed intensities



Emil J. Zak<sup>a</sup>, Jonathan Tennyson<sup>a,\*</sup>, Oleg L. Polyansky<sup>a,b</sup>, Lorenzo Lodi<sup>a</sup>, Nikolay F. Zobov<sup>b</sup>, Sergei A. Tashkun<sup>c</sup>, Valery I. Perevalov<sup>c</sup>

<sup>a</sup> Department of Physics and Astronomy, University College London, London WC1E 6BT, UK

<sup>b</sup> Institute of Applied Physics, Russian Academy of Sciences, Ulyanov Street 46, Nizhny Novgorod 603950, Russia

<sup>c</sup> V.E. Zuev Institute of Atmospheric Optics, SB RAS, 1, Academician Zuev Square, Tomsk 634021, Russia

## ARTICLE INFO

### Article history:

Received 12 September 2016

Received in revised form

23 November 2016

Accepted 24 November 2016

Available online 7 December 2016

## ABSTRACT

Remote sensing experiments require high-accuracy, preferably sub-percent, line intensities and in response to this need we present computed room temperature line lists for six symmetric isotopologues of carbon dioxide: <sup>13</sup>C<sup>16</sup>O<sub>2</sub>, <sup>14</sup>C<sup>16</sup>O<sub>2</sub>, <sup>12</sup>C<sup>17</sup>O<sub>2</sub>, <sup>12</sup>C<sup>18</sup>O<sub>2</sub>, <sup>13</sup>C<sup>17</sup>O<sub>2</sub> and <sup>13</sup>C<sup>18</sup>O<sub>2</sub>, covering the range 0–8000 cm<sup>−1</sup>. Our calculation scheme is based on variational nuclear motion calculations and on a reliability analysis of the generated line intensities. Rotation–vibration wavefunctions and energy levels are computed using the DVR3D software suite and a high quality semi-empirical potential energy surface (PES), followed by computation of intensities using an *ab initio* dipole moment surface (DMS). Four line lists are computed for each isotopologue to quantify sensitivity to minor distortions of the PES/DMS. Reliable lines are benchmarked against recent state-of-the-art measurements and against the HITRAN2012 database, supporting the claim that the majority of line intensities for strong bands are predicted with sub-percent accuracy. Accurate line positions are generated using an effective Hamiltonian. We recommend the use of these line lists for future remote sensing studies and their inclusion in databases.

© 2016 Published by Elsevier Ltd.

## 1. Introduction

Remote sensing of carbon dioxide for atmospheric applications requires a detailed knowledge of the rotational–vibrational spectra of all its major isotopologues. It is commonly believed that such measurements should be supported by reference line intensities of 1% accuracy or better [1]. This is the main requirement for successful interpretation of data from the NASA Orbiting Carbon Observatory 2 (OCO-2) space mission, which is designed to monitor the concentration of carbon dioxide in Earth's atmosphere. As was shown in our previous papers considering the main <sup>12</sup>C<sup>16</sup>O<sub>2</sub> isotopologue (denoted here as 626), a fully *ab initio* dipole moment surface is capable of providing such a level of accuracy [2,3]. The next step is to address other isotopologues, which are ubiquitous in natural samples and may interfere with spectral lines of the main isotopologue as well as other species [4–7]. Concentration measurements of trace compounds also require very accurate line positions, intensities and line profiles of several isotopologues at the same time.

Experimental line-intensity measurements for isotopologues

other than the main 626 one are much more challenging due to their low natural abundance, which ranges from 1% for <sup>13</sup>C<sup>16</sup>O<sub>2</sub> (636) down to 10<sup>−10</sup>% for the unstable <sup>14</sup>C<sup>16</sup>O<sub>2</sub> (646). Enriched samples feature the need for precise (*a priori*) knowledge of isotopologue concentration. Therefore experimental accuracies of line intensities for less abundant isotopologues of carbon dioxide are in general lower than for the main isotopologue. A comprehensive source of spectroscopic data for carbon dioxide is the HITRAN database [8]. The 2012 release of this database contains line lists for the <sup>13</sup>C<sup>16</sup>O<sub>2</sub> (636), <sup>12</sup>C<sup>17</sup>O<sub>2</sub> (727), <sup>12</sup>C<sup>18</sup>O<sub>2</sub> (828) and <sup>13</sup>C<sup>18</sup>O<sub>2</sub> (838) isotopologues, all featuring spectral gaps because of lack of experimental data. Line intensities included in the database have uncertainties of 5–20%, thus well above current requirements. The database comprises both semi-empirical (taken from the pre-release of the CDSD database [9,10]) and purely experimental entries. Multiple data sources are reflected by discontinuities in intensity patterns of some bands [3]. Several measurements have been made since the last edition of the database, to pursue the elusive naturally abundant molecules, although these studies also have uncertainties well above the desired 1% threshold. The most accurate recent experiments by Devi et al. [11], Jacquemart et al. [12–15], Karlovets et al. [5] and Durré et al. [16] address several bands of carbon dioxide isotopologues with unprecedented, though still unsatisfactory, intensity

\* Corresponding author.

E-mail address: [j.tennyson@ucl.ac.uk](mailto:j.tennyson@ucl.ac.uk) (J. Tennyson).

accuracies between 1% and 20%.

Among the few theoretical attempts to model high-resolution infrared spectra of carbon dioxide, the study by Huang et al. from the NASA Ames Research Center proved to be very accurate [17,18]. Line lists from Huang et al. provide both line positions and intensities covering the infrared and visible spectral region ( $J = 0$ –150) for room temperature (296 K) and 1000 K. Line positions, derived from a variational approach and based on semi-empirical potential energy surface (PES), are accurate to  $0.03$ – $0.2\text{ cm}^{-1}$ . Although the Ames-1 line lists [17,18] show the best agreement with experiment among all variational calculations, semi-empirical approaches based on effective Hamiltonians can provide line positions with an accuracy at least one order of magnitude better [9]. On the other hand, effective Hamiltonian models strongly depend on the quality of the input data, thus the accuracy and completeness of this technique are limited by experiment.

A major advantage of the use of variational nuclear motion programs is that, within the limits of the Born–Oppenheimer approximation, line intensities can be computed with the same accuracy for all isotopologues. In the present study the computation of line intensities was based on *ab initio* dipole moment surfaces (DMSs), and these were preliminarily tested by several authors [3,10,11]. Some minor inaccuracies and discontinuities were discovered; however, comparisons showed overall good agreement with experiment. A comprehensive literature review on both experimental and theoretical approaches to line positions and intensities is given in the recent work by Tashkun et al. [10]. In this study the authors indicate and support the need for a unified theoretical treatment of line positions and intensities; whereas the former are largely covered by experiments facilitated by effective Hamiltonian models [9], the latter still await high levels of accuracy, which we target in the present study. Due to lack of experimental data, a line list for the radioactive isotopologue  $^{14}\text{C}^{16}\text{O}_2$  is not included in the HITRAN2012 and CDS-296 databases. The Ames-1 line list is presently a unique source of high accuracy spectra for this species.

The unstable  $^{14}\text{C}^{16}\text{O}_2$  isotopologue is of particular importance because of its usage in dating of biosamples and, more recently, in monitoring emissions, migrations and sinks of fossil fuel combustion products [19–21] as well as for the assessment of contamination from nuclear power plants [22]. Until recently, monitoring fossil fuel emission relied mostly on  $\beta$ -decay count measurements or mass spectrometry, both of which are high cost, invasive methods.

Despite its low natural atmospheric abundance, radiocarbon dioxide has been probed via optical spectroscopy methods [6,7,23,24]. Recent advances in absorption laser spectroscopy provided an unprecedented tool for detection of species containing radiocarbon of ratios  $^{14}\text{C}/^{12}\text{C}$  down to parts per quadrillion. These measurements exploit saturated-absorption cavity ring down (SCAR) spectroscopy technique [25] for the strongest fundamentals of  $^{14}\text{CO}_2$  [7,24]. The knowledge of accurate line intensities for several isotopologues at the same time is therefore a necessity for eliminating the unwanted noise sourced in traces of different isotopic carbon dioxide representatives. For instance the  $P(20)$  line of the 00011–00001 band in 646, which is dedicated for radiocarbon measurements, above certain temperatures, heavily interferes with the Lorentzian tail of the  $P(19)$  line in the 05511–05501 band of the 636 isotopologue [4]. This raises difficulties in retrieving unbiased concentrations of the radioactive isotopologue. Similar problems occurred in measurements based on the  $P(40)$  line of the  $\nu_3$  band of  $^{14}\text{CO}_2$  [26]. In both cases accurate values of line intensities are required. Otherwise, as shown in [26], calculation of the fraction of  $^{14}\text{C}$  in measured samples that employed a line strength taken from a theoretical approach, led to over 35% error in retrieved concentrations (as later confirmed by

alternative experiments (AMS)). These observations were explained in terms of both inaccuracies of the line intensity and drawbacks of the spectroscopic fit model used, which fuels the need for reliable line intensity sources. Another successful technique further supporting this need was recently introduced by Genoud et al. [6], cavity ring-down spectroscopy with quantum cascade laser for monitoring of emissions from nuclear power plants. High quality line intensities for  $^{12}\text{C}^{16}\text{O}_2$ ,  $^{13}\text{C}^{16}\text{O}_2$  and  $^{16}\text{O}^{12}\text{C}^{18}\text{O}$  are also required for real-time detection methods based on quantum cascade lasers to monitor  $^{13}\text{C}/^{12}\text{C}$  isotope ratios in identification of bio-geo-chemical origins of carbon dioxide emissions from the soil–air interface [27].

Spectra of isotopologues can be used for a variety of different tasks such as the recent suggestion that observations of absorptions by  $^{13}\text{CO}_2$  in breath analysis provides a non-invasive means of diagnosing gastrointestinal cancers [28].

In this work we aim to provide highly accurate line intensities in the  $0$ – $8000\text{ cm}^{-1}$  spectral region together with reliable semi-empirical line positions for six symmetric isotopologues of carbon dioxide; five naturally abundant: 636, 727, 737, 828, 838 and one radioactive (646). An important advantage of a first principles theoretical approach is wide spectral coverage, in contrast to limited laser tuning capability of some measurements. For this reason databases like HITRAN, containing ro-vibrational spectra of small molecules, often utilize various experimental data sources, thereby giving up consistency of entries. This is not the case for the *ab initio* approaches, which are believed to provide consistent accuracy of line intensities within a vibrational band [29].

Another issue related to post-processing of experimental data is the functional form of the Herman–Wallis factors. These, as arbitrarily chosen and empirically fitted, can become a source of unnatural biases for high  $J$  transitions [3]. The theoretical model implemented here should be inherently free from this problem, as the rotational contribution to line intensities is computed directly. The only underlying source of errors within the Born–Oppenheimer approximation is potential energy surface (PES) and dipole moment surface (DMS). The quality of both surfaces is assessed here by employing the line sensitivity analysis procedure introduced by Lodi and Tennyson [29], which requires computation of at least four line lists for each isotopologue. This allows us to detect resonances [3] that affect line intensities and significantly diminish the reliability of data provided.

The final results are given in the form of line lists with associated uncertainties, which are available in the supplementary materials. Uniformity of errors (except for the regions affected by resonance interactions) accompanied by the precise reproduction of observed line intensities at the sub-percent level for the majority of strong bands [3] suggests that our results provide a viable update to the current, 2012 version of the HITRAN database.

## 2. Methodology

The Lodi–Tennyson methodology presented in detail elsewhere [3,29] is used to validate line lists on a purely theoretical basis. For each isotopologue four line lists were computed, based on set of two PESs and two DMSs. These surfaces come from two sources: the semi-empirical Ames-1 PES and DMS from Huang et al. [17], an *ab initio* PES and DMS (UCL DMS) computed by us, where the former one was subsequently fitted to observed  $J = 0$ – $2$  levels (called below: Fitted PES). Details of all surfaces were presented before [3]. These four high-quality surfaces are used in nuclear motion calculations to obtain rotational–vibrational energy levels, wavefunctions and line intensities.

## 2.1. Nuclear motion calculations

The strategy for solving the nuclear-motion problem employed here is analogous to the one presented in [3]. In the Born–Oppenheimer approximation the PES and DMS are isotopologue independent. Therefore the only parameters that distinguish between different isotopologues are the nuclear masses entering the expression for the kinetic energy operator (KEO) of the nuclei. Our approach is based on an exact, within the Born–Oppenheimer approximation, KEO which is used in a two step procedure [30–32] of solving the nuclear Schrödinger equation. The first step involves solving the Coriolis-decoupled ro-vibrational motion problem for every ( $J$ ,  $lkl$ ) quantum number combination separately to supply a basis for the second step, where the full ro-vibrational Hamiltonian is considered. The DVR technique implemented in the DVR3D suite [33] is used to represent the Hamiltonian matrix. Diagonalization of this matrix provides rotational–vibrational energy levels and wavefunctions. In the present study we used symmetrized Radau coordinates and a bisector embedding to define nuclear degrees of freedom in the body-fixed coordinate system.

Nuclear masses for isotopes of carbon and oxygen were used: 11.996709 Da ( $^{12}\text{C}$ ), 13.000439 Da ( $^{13}\text{C}$ ), 14.000327 Da ( $^{14}\text{C}$ ), 15.990525 Da ( $^{16}\text{O}$ ), 16.995245 Da ( $^{17}\text{O}$ ) and 17.995275 Da ( $^{18}\text{O}$ ) [34]. In the first step of the computation (program DVR3DJZ) the Born–Oppenheimer ro-vibrational wavefunctions were expanded in Morse-like oscillator basis functions for stretching coordinates and Legendre polynomials for the bending one; symmetrized Radau internal coordinates were used. The converged DVR basis set associated with Gauss–Legendre quadrature points contained 30 radial and 120 angular functions, respectively. In the second step (program ROTLEV3b) we employed a  $J$ -dependent basis set of symmetry-adapted symmetric-top rotational functions. The  $J$  ranges considered were chosen to match those present in the HITRAN2012 database (see Table 1). The same set of parameters was used to evaluate ro-vibrational energies computed from Ames-1 and fitted PESs. Calculation of line strengths used the DIPOLE program and requires both DMS and ro-vibrational wavefunctions as input functions. Transformation from line strengths to transition intensities included scaling by natural isotopic abundance and multiplication by the appropriate spin statistical weights. Partition functions at 296 K were taken from Huang et al. [17] and they agree to better than 0.1% with partition functions from the present computation based on Ames-1 PES (see Table 1). A natural-abundance weighted intensity cut-off was then set to

$10^{-30}$  cm/molecule. In the case of the radioactive isotopologue (646) we assumed unit abundance and increased the cut-off value to  $10^{-27}$  cm/molecule.

## 2.2. Estimation of the intensity uncertainties

The *ab initio* DMS is a primary source of inaccuracies in line intensities. The accuracy of the UCL DMS has been proven to be at sub-percent level for several strong bands (stronger than  $10^{-23}$  cm/molecule) below  $8000\text{ cm}^{-1}$  [2,3]. A key feature of using an *ab initio* DMS with a variational nuclear motion calculation for 626 is that entire vibrational bands are reproduced with similar accuracy. The reliability of line intensities obtained theoretically is correlated with the quality of  $J$ -dependent ro-vibrational wavefunctions, hence with an underlying PES. Wavefunctions play an important role in capturing the interaction between different vibrational states. Such resonance interactions can lead to intensity stealing and, particularly for the so-called dark states, huge changes in transition intensities.

Indeed, the sensitivity analysis performed for 626 [3] indicated that certain ro-vibrational energy levels of  $\text{CO}_2$  are vulnerable to interactions induced by Coriolis-type terms in the Hamiltonian. These resonances may change intensities of lines, particularly for weak transitions, by several orders of magnitude. This effect manifests itself especially when the perturbing band is strong. For this reason even minor inaccuracies in the PES in regions where such interactions occur can significantly change the intensity of lines, hence not reflecting the accuracy of the DMS. Thus, it is important to filter out bands or specific transitions with perturbed intensities which should not be trusted. A few such bands have been reported for the main isotopologue of  $\text{CO}_2$  (626) [3,35] and other isotopologues [5,14,15].

Here we adopt a scheme from our previous works [3,29], where a method of locating resonances was developed and tested on  $\text{H}_2\text{O}$  and  $^{12}\text{C}^{16}\text{O}_2$ . Cross-comparison of four line lists yielded an intensity scatter factor  $\rho$  assigned to every line, which is defined as the ratio of the strongest to the weakest transition in a set of four intensities matching the same transition line. The four line lists read: Ames-1 PES and Ames DMS (named AA), Ames-1 PES and UCL DMS (named AU), Fitted PES and Ames DMS (named FA), Fitted PES and UCL DMS (named FU). Our base model, which should on theoretical grounds be the most accurate, is AU; it is from this model that our underlying uncertainties are drawn. For transitions involved in resonance interactions, calculations with

**Table 1**  
General information on computed room temperature ( $T=296\text{ K}$ ) line lists.

Isotopologue	636	646	727	737	828	838
ZPE <sup>a</sup> ( $\text{cm}^{-1}$ )	2483.08	2436.75	2500.75	2447.50	2469.05	2415.39
$J_{\text{MAX}}$	119	130	99	50	101	50
Spin factors (ortho:para)	2:0	7:0	15:21	30:42	1:0	2:0
$Q_{296}$ (This work)	576.652	2033.395	10 902.24	21 758.08	323.438	644.754
$Q_{296}$ (CDSD-296) <sup>b</sup>	576.652	N/A	10 971.90	22 129.96	323.418	652.234
$Q_{296}$ (Ames-296) <sup>c</sup>	576.644	2033.353	10 971.91	22 129.96	323.424	652.242
$Q_{296}$ (HITRAN) <sup>d</sup>	578.408	N/A	11 001.67	N/A	324.211	653.756
Abundance <sup>e</sup>	0.011057	1.0	$0.13685 \times 10^{-6}$	$0.15375 \times 10^{-8}$	$0.39556 \times 10^{-5}$	$0.44440 \times 10^{-7}$
No. lines (This work) <sup>f</sup>	68 635	41 610	6530	1501	10 441	2637
No. lines (CDSD-296) <sup>f</sup>	68 640	N/A	6530	1500	10 444	2635
No. lines (Ames-296) <sup>f</sup>	68 739	42 072	6545	1634	10 531	3050
No. HITRAN lines	68 856	N/A	5187	N/A	7070	121
No. HITRAN matches <sup>g</sup>	68 856	N/A	5187	N/A	7069	121

<sup>a</sup> Zero point energy based on the Ames-1 PES.

<sup>b</sup> 2015 Edition of CDSD [10].

<sup>c</sup> Ref. [17].

<sup>d</sup> TIPS-2011 [43].

<sup>e</sup> HITRAN2012 abundances were taken from Ref. [17].

<sup>f</sup> For  $10^{-27}$  cm/molecule intensity cut-off for the 646 isotopologues and  $10^{-30}$  cm/molecule after scaling for natural abundance for the other isotopologues.

<sup>g</sup> UCL-IAO line list with  $10^{-33}$  cm/molecule intensity cut-off was used in the comparison.

different procedures should give markedly different results. The trustworthy line intensities should be stable under minor PES/DMS modifications, hence should feature a small scatter factor. Based on the statistics of the scatter factor we established arbitrary limits on  $\rho$  for a line to be considered stable ( $1.0 \leq \rho < 2.5$ ), intermediate ( $2.5 \leq \rho < 4.0$ ) and unstable ( $\rho \geq 4.0$ ). These values are the same for all isotopologues. We believe that this descriptor gives a robust measure of sensitivity of line intensities to small PES changes, and hence reflects the reliability of a theoretically evaluated line intensity.

### 2.3. Line positions

As discussed above line positions for the recommended UCL-IAO line list are taken from the CDSD-296 database [10]. These line positions were calculated within the framework of the effective Hamiltonian approach for which the partly reduced polyad model was used [36–38]. This model takes into account the resonance anharmonic, anharmonic+ $l$ -type and Coriolis interactions. The global weighted fits of the effective Hamiltonian parameters to the observed line positions collected from the literature were performed. The observations cover the  $0.7$ – $13\,633\text{ cm}^{-1}$  range, but for the rare isotopologues the ranges of the observations are considerably smaller. A review of the observed line positions used is given elsewhere [10]. Each isotopologue was considered separately. In the case of isotopologues for which the observed line positions are scarce the effective Hamiltonian parameters obtained from the multi-isotopologue fitting [39] were used as an initial guess for further refinement of some of the parameters by separate fitting. The fitted sets of the effective Hamiltonian parameters reproduce the observed line positions practically within their experimental uncertainties, from  $10^{-9}\text{ cm}^{-1}$  to  $0.01\text{ cm}^{-1}$ . The good predictive ability of the resulting effective Hamiltonian parameters has been demonstrated many times [5,12–14,40,41]. The exceptions are several bands of the asymmetric isotopologues which are perturbed by the interpolyad resonance anharmonic interactions. Some of the examples are given in Refs. [5,40,41]. Usually these perturbed bands are very weak.

### 2.4. Pseudo-experimental refinements

Energy levels taken from the effective Hamiltonian (EH) are generally considered to be accurate to  $0.002\text{ cm}^{-1}$  or better, which is usually more accurate than those given by PES based studies [10]. Multi-isotopologue fits allowed for completeness of EH line lists even for less abundant isotopologues [42]. From this reason our recommended line lists include line positions from the Effective Hamiltonian calculations provided by the CDSD-296 database [10]. However, the very limited experimental data for  $^{14}\text{C}^{16}\text{O}_2$  did not allow us to extract EH parameters for this isotopologue. Therefore an alternative source of line positions is needed here.

Comparison of DVR3D (AMES-1 PES) line positions with EH values for the  $^{13}\text{C}^{16}\text{O}_2$  isotopologue shows that on average agreement between the two is at the  $0.02\text{ cm}^{-1}$  level. Within one vibrational band the residuals between EH and DVR entries remain almost constant. This observation suggests the viability of correcting the DVR3D line positions with respective differences for the main isotopologue. Such an approach has recently been shown to give excellent results for  $\text{H}_2^{18}\text{O}$  and  $\text{H}_2^{17}\text{O}$  [29].

Thus, an attempt to correct DVR3D line positions with the effective Hamiltonian values was made. First, energy differences between corresponding EH and DVR energy levels for the main isotopologue were taken:  $\Delta E(626) = E_{\text{EH}}^{626} - E_{\text{DVR}}^{626}$ . Next, each energy level of a given less abundant isotopologue was refined by adding respective difference to the DVR-computed value:

$E^{\text{ISO}} = E_{\text{DVR}}^{\text{ISO}} + \Delta E(626)$ . These refined energy levels were then compared to EH values. Application of the above procedure to symmetric isotopologues of  $\text{CO}_2$  resulted however in increased deviations between DVR and EH energy levels, hence should be considered here as unsuccessful. The reason for this is not entirely clear but the cited study for water [29] took considerable care over the corrections to the Born–Oppenheimer approximation while the results here were based on a PES simultaneously fitted to data from several isotopologues with no allowance for the beyond Born–Oppenheimer effects. For this reason pure DVR3D line positions were used in the recommended line list for  $^{14}\text{C}^{16}\text{O}_2$ .

## 3. Results and discussion

Below we present an overview of our line lists. The next subsection contains statistical analysis of the scatter factor for each isotopologue, which will be further used in detecting resonances in the following subsection. After that, we compare our present results to recent highly accurate measurements, which were not included in the latest release of the HITRAN database. Next, a detailed comparison with the HITRAN2012 and CDSD-296 databases is performed. Finally we discuss the radioactive 646 isotopologue in the environmental context, as one of the possible applications of present results.

### 3.1. Overview

Table 1 contains general information about our line lists.

Partition functions in this work were calculated using Ames-1 PES, and these are compared to HITRAN2012, Ames and CDSD-296 line lists. We can see from Table 1 that for isotopologues: 636, 646 and 828 the agreement between Ames work and our values is at 0.002% level, as expected from runs based on the same PES. Partition functions calculated by us should however be treated as provisional for the 737 and the 838 isotopologue, as  $J$ -range employed here did not allow for full convergence of the partition function. On average, the computed partition functions agree excellent with CDSD-296, and are systematically shifted by  $-0.3\%$  with respect to HITRAN2012. This fact must be taken into account in comparisons aimed at sub-percent accuracy of line intensities. For line intensity calculations we used Ames partition functions from Huang et al. [17]. The HITRAN2012 database has significant spectral gaps for less abundant isotopologues, which are all covered by our line lists. Lines present in HITRAN2012 were completely matched to our lines using the energy level comparison technique.

### 3.2. Scatter factor statistics

Fig. 1 gives an overview of the scatter factor statistics for all isotopologues considered. It is readily seen that the majority of lines are classified as stable, that is have scatter factor less than 2.5 (marked in blue in Fig. 1). For  $^{13}\text{C}^{17}\text{O}_2$  and  $^{13}\text{C}^{18}\text{O}_2$  all lines are stable. Line lists for  $^{13}\text{C}^{16}\text{O}_2$  and  $^{14}\text{C}^{16}\text{O}_2$  have 3.5% and 3.3% of unstable lines respectively, whereas the  $^{12}\text{C}^{18}\text{O}_2$  line list features only 0.5% of unstable lines. Whenever a line-to-line match between a Fitted PES derived line and an Ames-1 based line was impossible by our automatic procedure due to ambiguity in matching of energy levels, manual attempts were made. Nevertheless a small fraction of lines remained unmatched, resulting in ‘unknown’ scatter factors; the number of such unmatched lines is small for all isotopologues. The blue dashed area denotes stable and strong lines ( $>10^{-23}\text{ cm}^2/\text{molecule}$ ), for which the most accurate HITRAN accuracy index was assigned ( $ier=8$ ). The HITRAN uncertainty index value ( $ier$ ) equal to 8 corresponds to accuracy of



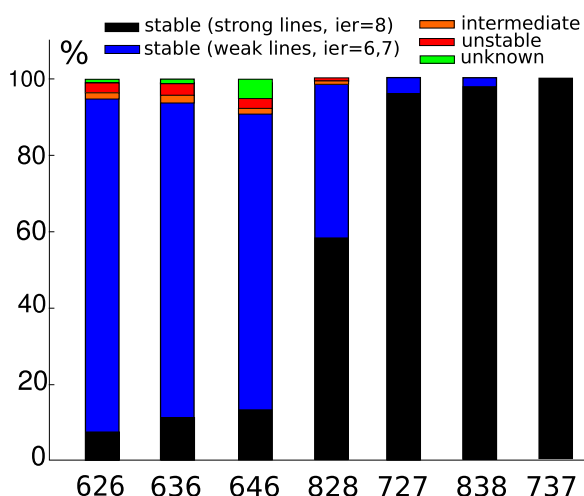


**Fig. 1.** Scatter factor statistics for six isotopologues of carbon dioxide. Respective colors denote percentages of lines classified to particular stability domain. The y-axis corresponds to percentage of total lines present in our line list. Black regions give percentage of stable and strong lines ( $>10^{-23}$  cm/molecule), for which the highest HITRAN intensity accuracy code was assigned ( $ier=8$ ). (For interpretation of the references to color in this figure caption, the reader is referred to the web version of this paper.)

line intensity better than 1%. Consequently,  $ier=7$  stands for 1–2% accuracy,  $ier=6$  stands for 2–5% accuracy,  $ier=5$  stands for 5–10% accuracy,  $ier=4$  stands for 10–20% accuracy and  $ier=3$  stands for line intensities accurate to 20% or worse.

### 3.3. Resonances

Detailed information on the energetic distribution of the scatter factor may be extracted from a ‘transition stability map’, which is a useful tool in searching for resonances, as exemplified in Fig. 2, which presents an example of such a map for the 828 isotopologue. The advantage of this particular representation is that one gains a full overview of all energetic regions, where transition intensities appear to be sensitive to minor inaccuracies of the PES. These lines are marked as red dots in Fig. 2.

Fig. 2 also illustrates the general trend of decreasing stability of lines with increasing energy of states involved in a transition. This has been already observed for the main 626 isotopologue in [3]. Sporadic red points localized in small energetic areas are indicative of  $J$ -localized resonances, while long chains of unstable

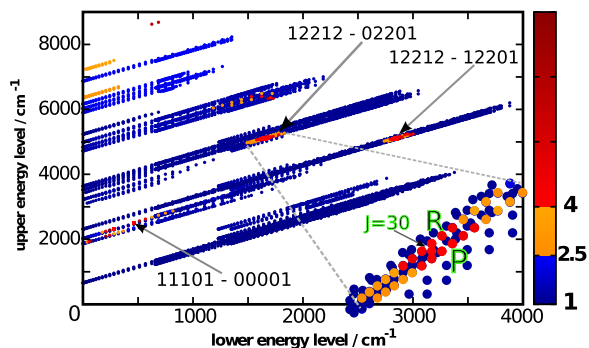


**Fig. 2.** Scatter factor map for the 828 isotopologue. Color coding denotes respective classification of lines: blue stands for stable lines, orange for intermediate lines and red for unstable lines. The arrows indicate selected bands for which a  $J$ -localized peak in the scatter factor is observed. The zoomed inset in right bottom corner shows the peak region of the scatter factor for the 12212–02201 band. Both P and R branches are affected by the interaction around  $J=30$ . (For interpretation of the references to color in this figure caption, the reader is referred to the web version of this paper.)

points suggest instability of whole bands. It is instructive to give a more detailed insight into resonances by plotting scatter factor as a function of  $m$  quantum number for each band separately within a given polyad number change ( $\Delta P$ ). The  $m$  quantum number is defined as equal to  $-J$  (lower energy level) for the P branch,  $J$  (lower energy level) for the Q branch, and  $J$  (lower energy level) + 1 for the R branch. The polyad number for carbon dioxide is defined as  $P = 2\nu_1 + \nu_2 + 3\nu_3$ , where  $\nu_1, \nu_2, \nu_3$  are the vibrational quantum numbers of symmetric stretching, bending and asymmetric stretching, respectively.

In general bands with polyad number change equal to 1 ( $\Delta P = 1$ ) are stable. For  $\Delta P = 3$  three unstable bands were found: 23301–12202, 11101–00001 and 11102–00001. The first of the three bands contains transitions for which upper energy levels (localized around a particular  $J$  value) become energetically close to rotational states of some other vibrational state; in this case to levels from the 12212 state. This may lead to a strong resonance interaction between states. In the case of the last two bands, an intensity borrowing mechanism from the strong asymmetric stretching fundamental is responsible for the instability of line intensities around a particular  $J$  (see Figs. 3 and 5). For  $\Delta P = 5$ , both 12212–02201 and 23301–02201 bands are subject to a  $J$ -localized resonance, as depicted in Fig. 6. This is due to mutual interaction of the upper levels of these bands, which are energetically close. For  $\Delta P = 7$ , the 22213–02201 band exhibits a weak  $J$ -localized peak in the scatter factor around  $J=34$ . The 31101–00001 band is weakly perturbed by interaction between the 31101 and 20012 states in the vicinity of  $J=68$ . Bands with higher polyad change number ( $\Delta P = 9, 11$ ) are in general less stable, following uniform distribution of the scatter factor.

Resonances occur when ro-vibrational energy levels of two or more states cross or nearly cross in the vicinity of a single  $J$  value. A prominent example of near crossing situation is the 11101–00001 band, which is perturbed by the 00011 state (intrapolyad interaction). Because the 00011–00001 fundamental is very strong and the perturbed band is relatively weak, significant intensity stealing is observed. This case is depicted in Fig. 4. The relative intensity representation supplied by Fig. 4 leads to the immediate conclusion of unreliability on the theoretical line intensities of transitions affected by resonances.

In Fig. 4 color coding shows the stability of the transition intensity. A  $J$ -localized resonance is visible around  $m=+36$ , clearly correlating with both high instability of lines (marked by red points) and large deviations from HITRAN2012 line intensities.

This quasi-singularity in line intensity occurs due to Coriolis interaction with the strong 00011–00001 band, which equally perturbs P and R branches of the 11101–00001 band, and

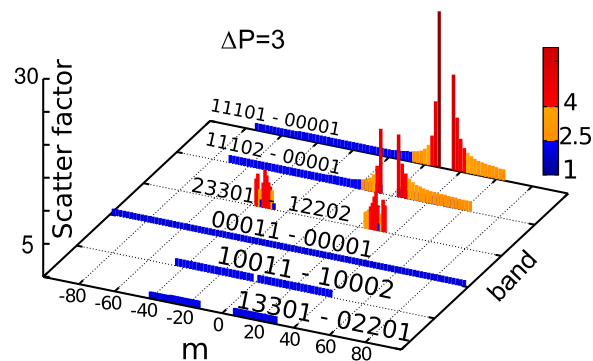


**Fig. 3.** Scatter factor distribution for selected bands of 828 with polyad change  $\Delta P = 3$ . Color code denotes classification of transition as stable (blue), orange (intermediate) or unstable (red), measured by the scatter factor. (For interpretation of the references to color in this figure caption, the reader is referred to the web version of this paper.)

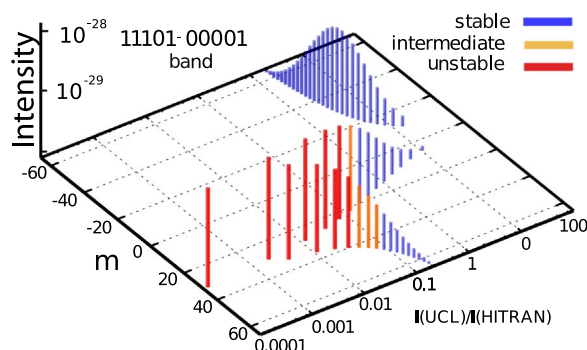


**Fig. 4.** Relative intensities plotted against HITRAN2012 line intensities for the 11101-00001 band for the 828 isotopologue. This is an example of a band involved in resonant Coriolis interaction. Blue, orange and red points denote stable, intermediate and unstable lines, respectively. (For interpretation of the references to color in this figure caption, the reader is referred to the web version of this paper.)

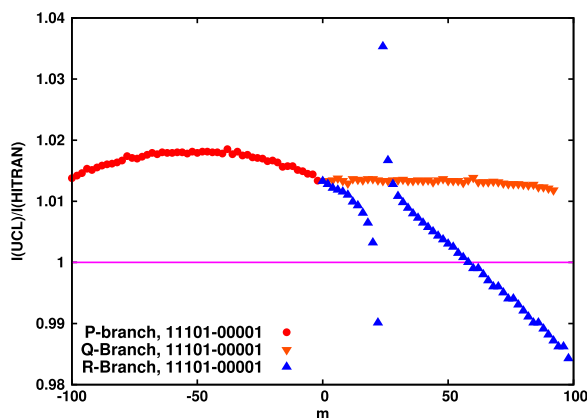
manifests itself by intensity borrowing, which in turn leads to the strengthening of the P-branch and to suppression of the R-branch. This observation confirms our previous predictions for existence of such perturbation in the main isotopologue [3]. For this reason, in the final recommended line list we replace line intensities perturbed by these Coriolis interactions with semi-empirical data from the CDSD-296 database.

A view of the 636 isotopologue in Fig. 5 supports this thesis. Similar behavior is observed for other isotopologues. The 636 case clearly shows that this type of interaction is branch-specific and  $J$ -specific as illustrated in Fig. 5.

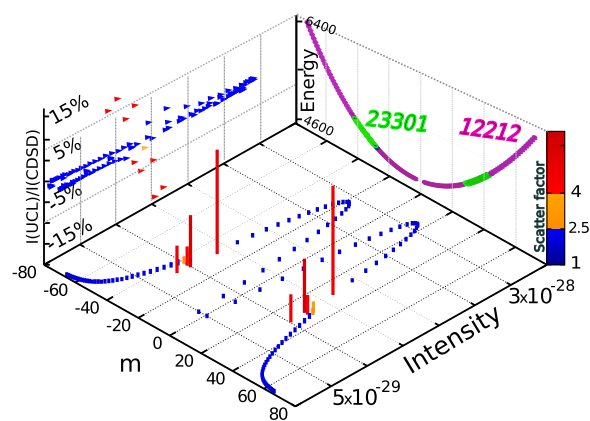
Another example of the intrapolyad interaction is the pair: 23301 (perturber) and 12212-02201 (perturbed band), for which we depict the intensities scheme in Fig. 6.

Fig. 6 shows perfect correlation between line stability measured by the scatter factor and agreement with CDSD-296 line intensities, where large discrepancies surround the region of elevated scatter factor (marked with red filled triangles in Fig. 6). Very similar behavior for line positions of the 12212-02201 band was noted by Borkov et al. for 727 [14], whose simple polynomial fit of the line positions resulted in a  $J$ -localized quasi-singularity in deviation of line positions. In such cases, effective Hamiltonian calculations have proved to be very successful and should be trusted regardless of resonances [5,15].

One would expect that at least some of the large deviations in line intensities (see Figs. 5 and 6) can be assigned to the influence of a resonance. Indeed, the correlation between high deviations in intensity and high scatter factor values is strikingly high, and re-



**Fig. 5.** Relative intensities plotted against HITRAN2012 line intensities for 11101-00001 band for the 636 isotopologue. This is an example of a band involved in resonant Coriolis interaction.



**Fig. 6.** Multidimensional graph characterizing the 12212-02201 band of  $^{12}\text{C}^{18}\text{O}_2$ . The base plane depicts  $m$  dependence of line intensities with bar height and color code measuring the value of the scatter factor. The far right plane represents  $m$  dependence of energy levels of the perturbed state (12212) and perturber (23301), which happen to nearly overlap around  $m = \pm 36$ . Left plane gives intensity ratios of lines taken from UCL line list and CDSD-296 database. (For interpretation of the references to color in this figure caption, the reader is referred to the web version of this paper.)

liability of the data provided might be unresolvable in favor of either approach. Nevertheless, as many HITRAN2012 transitions come from CDSD-296 semi-empirical calculations, one should expect them to be trustworthy. This behavior is common for all bands in our line lists. Therefore we may consider the scatter factors used as a legitimate measure of reliability of a theoretical line list.

In the recommended line lists given in the supplementary materials, we replace the intensities of lines identified as unstable with entries from the effective Hamiltonian calculations, which for these cases are much more reliable, being experimentally based. Line lists with *ab initio* intensities can be found in supplementary material in files named as 'UCL-IAO-296-isotopologue\_name.dat'.

### 3.4. Comparison with recent measurements

Numerous experimental line intensity data sources are available throughout the literature (see Refs. [10,44] for a comprehensive review), of which only few have high precision. Our attention is therefore focused on the most recent and the most accurate measurements. We assume that up to 2011 all highly accurate measurements and computations are captured by the 2012 edition of HITRAN, which will be analyzed below.

A notable advantage of our *ab initio* approach is constant accuracy of intensity of entire bands, which is also believed to be transferable between different isotopologues. This is because all line intensities are computed using the same PES and DMS. Assuming that non-Born–Oppenheimer corrections are negligible we should expect an accuracy of 1% or better for strong and stable bands of all symmetric isotopologues. These bands are defined as ones containing transitions stronger than  $10^{-23}$  cm/molecule at 100% abundance. For the weak stable and intermediate bands this accuracy reduces to 1–3%. Such levels of accuracy are generally beyond reach of current experimental techniques, especially for the less abundant species.

### 3.5. Isotopologue 636

Recently Devi et al. [11] performed precise measurements of line intensities of the 626, 636 and 628 isotopologues of carbon dioxide in the 1.6  $\mu\text{m}$  region. Fig. 7 compares our results and HITRAN2012 line intensities to these new experimental results. The HITRAN2012 data comes from the CDSD database. A significant

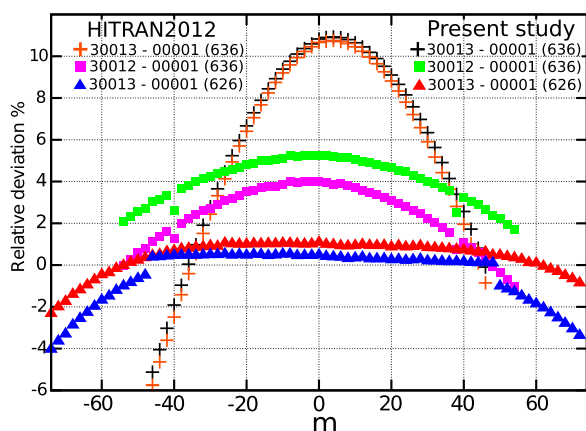


**Fig. 7.** Relative deviations (PS/Experiment) of line intensities from measurements by Devi et al. [11] plotted against  $m$  quantum number. Blue and red triangles denote the 300013–00001 band of the 626 isotopologue taken from HITRAN2012 and present study, respectively. Purple and green squares stand for line intensities of the 30012–00001 band of the 636 isotopologue taken from HITRAN2012 and present study, respectively. Orange and gray crosses give the line intensities of the 30013–00001 band of the 636 isotopologue taken from HITRAN2012 and present study, respectively. Zero relative deviation means 100% agreement with Devi et al. (For interpretation of the references to color in this figure caption, the reader is referred to the web version of this paper.)

systematic shift of 5% and 10% toward higher intensities is observed for both 30012–00001 and 30013–00001 band. An almost identical pattern is followed by our line intensities and the effective Hamiltonian calculations given under HITRAN2012 entries. Possible problems in measured line intensities were found at  $m=+38$  and  $m=-40$ . These transitions clearly stand out in the comparison pattern for both HITRAN and the present study. High  $J$  tails of both bands are bent in a bow-like structure, behavior which has been already observed for the main isotopologue. We attribute such behavior to limited flexibility of functional form assumed for the Herman–Wallis factors, when reducing the experimental data.

Less pronounced deviations in high  $J$  region have been observed in the work by Benner et al. [45], where highly accurate measurements for the 2.06  $\mu\text{m}$  band of the main isotopologue were made. Comparison shows 0.5% agreement between the experiment and UCL-IAO line intensities for the 20013–00001 band for the main isotopologue [45], and systematic increase in intensity deviation from  $m=60$  onwards to reach 1.5% deviation at  $m=84$ . Both experiments (Devi et al. [11] and Benner et al. [45]) utilized the same multispectrum nonlinear least squares curve fitting technique to retrieve line profiles and intensities. This similarity in high  $J$  behavior supports the thesis of potential problems with retrieval model used in experimental post-processing.

The accuracy of the experiments by Devi et al. and the present calculations has been verified by very recent Cavity Ring-Down Spectroscopy measurements of  $\text{CO}_2$  lines by Kiseleva et al. [46]. Their observed intensity of the P(6) line in the 30013–00001 band of the 636 isotopologue was found to be within 0.4% of both UCL and HITRAN line intensities. Further proof of the consistency between the experiment by Kiseleva et al. and the present study is the P(52) line of the 30014–00001 band of the main isotopologue (626), which was also compared and found to be only 0.17% from our predicted value. Both lines were measured with stated <1% uncertainty budget. This suggests that a similar, presumably sub-percent, accuracy for the line intensities provided here and by HITRAN2012 for the 30013–00001 band of the 636 isotopologue.

The 2010 experimental study by Durry et al. [16] deserves special attention, as intensity uncertainties for measured bands of the 636 isotopologue are claimed at the 1% level. Fig. 8 compares experimental line intensities from Durry et al. with HITRAN2004

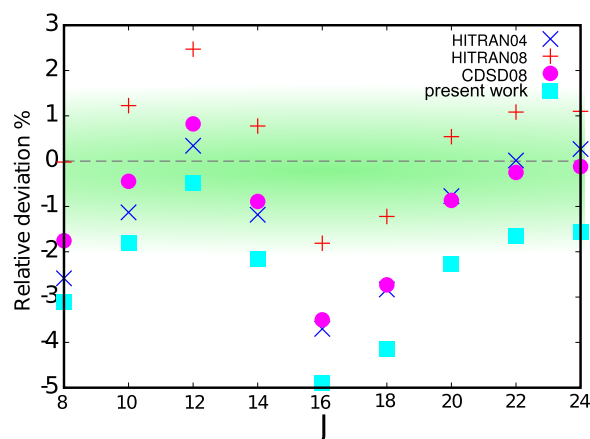


**Fig. 8.** Relative deviations of line intensities of the 20012–00001 band of the 636 isotopologue from measurements by Durry et al. [16] plotted against  $J$  quantum number for several databases. Sources considered are HITRAN2004 [47], HITRAN2008 [48], the 2008 release of CDSD [9] and the present work. The 1% deviation region is represented by green edge-blurred strip. (For interpretation of the references to color in this figure caption, the reader is referred to the web version of this paper.)

[47], HITRAN2008 [48] and 2008 release of the CDSD database [9,44], as well as with our calculated values. A characteristic wave-like pattern is visible. As all four sources follow this envelope, but with different systematic shifts, we conclude that this pattern is an artifact of the results of Durry et al. The points from present work are shifted toward most negative values of relative deviation, with average systematic shift of 2%. Intensity comparison for this band for the main 626 isotopologue [45] supports the 1% accuracy of our theoretical intensities. Therefore it would seem that the stated 1% uncertainty of Durry et al.'s measurements may be too optimistic.

### 3.6. Isotopologue 727

In recent measurements performed on  $^{17}\text{O}$  and  $^{18}\text{O}$  enriched samples, Jacquemart et al. [15] measured several bands for the 727 isotopologue. The authors argue that only lines stronger than  $10^{-25}$  cm/molecule are retrieved with 'good accuracy' and this accuracy is also strongly dependent on the knowledge of isotopic abundances. Fig. 9 compares intensities of different bands measured by Jacquemart et al. with our predictions. It is evident that lines weaker than  $1.0 \times 10^{-25}$  cm/molecule give reduced accuracy, as statistical spread appears to be an order-of-magnitude larger than for the strong bands measured in this experiment. Hence the

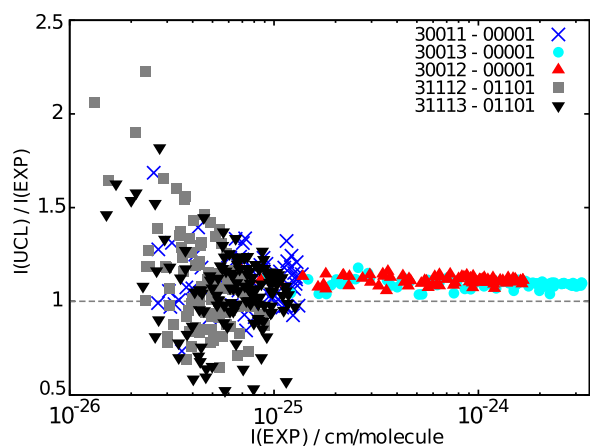


**Fig. 9.** Relative intensities for several bands of the 727 isotopologue measured by Jacquemart et al. [15]. (For interpretation of the references to color in this figure caption, the reader is referred to the web version of this paper.)

experimental results [15] for the 30011–00001, 31112–01101 and 31113–01101 band should be considered with caution.

The intensities of the two strongest bands in the 2  $\mu\text{m}$  region, that is 30012–00001 and 30013–00001, are uniformly shifted by +10% with respect to an experiment. As indicated by Jacquemart et al. [15], intensities of whole bands are strongly dependent on isotopologue abundance (reported as 22.27%), and this factor is considered to be the main source of possible systematic shifts with respect to other studies. Comparisons with previous measurements by Karlovets et al. [5] were made, revealing the new measurements by Jacquemart et al. [15] to be on average 3–4% stronger. However, samples used by Karlovets et al. had very low abundance of 727 (0.04%), which resulted in large statistical error (15%) in the intensities. Therefore we conclude that with the current level of experimental control over systematic errors it is difficult to reliably refer to measurements better than 10% accuracy. Nonetheless, because theoretical line intensities have constant accuracy for whole bands (except resonances), they can be used to assess the precision of measurements. Small scatter of line intensities throughout these bands (marked red and cyan in Fig. 9) confirms the claimed high precision (1%) of the measurement from Ref. [15] above  $\text{cm}/\text{molecule}$ , 2% between  $5 \times 10^{-25}$  and  $2.5 \times 10^{-24}$ , 5% between  $1 \times 10^{-25}$  and  $5 \times 10^{-25}$ , and 20% below  $1.0 \times 10^{-25}$ .

Fig. 10 compares line intensities from the present work to the experimental data from Karlovets et al. [5]. The low isotopic abundance of samples used in experiments and large stated uncertainty (15%) means that the comparison despite its large scatter is satisfactory. As for other isotopologues, the 00031–00001 band computed by us has an underestimated intensity (gray squares in Fig. 10). Cyan and red points correspond to 30013–00001 and 30012–00001 bands, and these experimental points were used to relate the line intensities of these bands in the study by Jacquemart et al.

### 3.7. Isotopologue 828

Recent CW-Cavity Ring Down experiments for enriched sample of the  $^{12}\text{C}^{18}\text{O}_2$  isotopologue by Karlovets et al. [41] cover the spectral range of all previous measurements for  $\Delta P = 9$  transitions. The study comprises 2870 lines from 59 bands in the 5851–6990  $\text{cm}^{-1}$  region and was recorded for 25.45% abundance. Crude experimental data was fitted with an effective operator model to take into account another accurate experimental dataset from Toth et al. [49], which has been also included in the 2012 release of the

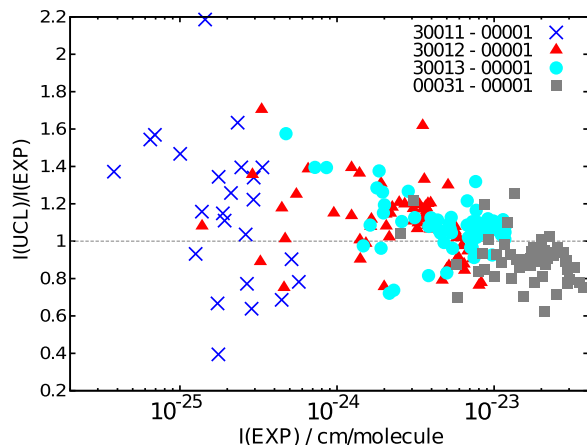


**Fig. 10.** Relative intensities for several bands of the 727 isotopologue measured by Karlovets et al. [5]. Intensities were scaled to unit abundance. (For interpretation of the references to color in this figure caption, the reader is referred to the web version of this paper.)

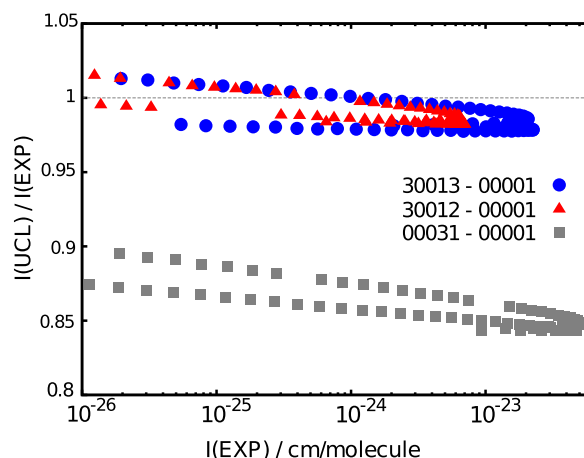


**Fig. 11.** Relative intensities for several bands of the 828 isotopologue measured by Karlovets et al. [41]. Intensities were scaled to unit abundance.

HITRAN database. The estimated 10% uncertainty of the line intensities is the most accurate claim up-to-date. For a detailed review of previous measurements for this isotopologue see Refs. [41,10] and references therein. Here, highly enriched sample allowed for more precise measurements than in the 727 isotopologue case. Fig. 11 compares line intensities of the three strongest bands measured by Karlovets et al. to present study. The 30012–00001 and 30003–00001 bands remain within  $\pm 2\%$  deviation range, which suggest that the stated experimental uncertainty of 10% is actually too pessimistic. Our intensities for the 00031–00001 band are shifted down by 14%, similar to other isotopologues. The recommended line list uses line intensities from CDSD-296 for this band.

Above results for 636, 727 and 828 isotopologues are summarized in Table 2.

### 3.8. Comparison with HITRAN2012, Ames and CDSD-296

The HITRAN2012 database comprises line lists for 636, 727, 828 and 838. Uncertainty indices of the line positions range from 2 ( $\geq 0.01 \text{ cm}^{-1}$  and  $< 0.1 \text{ cm}^{-1}$ ) to 9 ( $\geq 10^{-9} \text{ cm}^{-1}$  and  $< 10^{-8} \text{ cm}^{-1}$ ). In general, line positions from the latest version of CDSD-296 are very close to the line positions given in HITRAN2012 and have uncertainties corresponding to the indices ranging from 3 to 9 depending on spectral region and quality of underlying experimental entries. Intensities provided by the current release of HITRAN for symmetric isotopologues of carbon dioxide come from two main sources: experiment (JPL OCO line list) by Toth et al. [50] and the majority of transitions from a previous version of CDSD. The estimated uncertainties for all CDSD intensities are given as 20% or worse in HITRAN (uncertainty code 3). However, this number does not reflect the actual uncertainties of the intensities. Most of the HITRAN intensities have the uncertainties much better than 20%. More detailed information about the actual uncertainties can be found in the official release of CDSD [10], which can be used to get more realistic information about the uncertainties of the line parameters.

Intensities from Toth et al. are supposed to be accurate to better than 2% (uncertainty code 7) or 5% (code 6). As discussed elsewhere [3], the stated uncertainty estimates of all current entries are insufficiently accurate for remote sensing applications. In addition to that several bands feature unrealistic jumps in line intensities originating from switching data sources. Therefore a unified approach giving line positions of spectroscopic quality combined with significantly more accurate transition intensities is needed. In the present paper we aim in fulfilling these



**Table 2**

Characterization of selected vibrational bands of three symmetric CO<sub>2</sub> isotopologues. Given for each band and each reference are the number of lines in the band, accuracy declared in the reference, average systematic shift ( $\Delta_{\text{sys}} = \bar{S}$ : average residual with respect to present study), average statistical dispersion ( $\Delta_{\text{stat}} = \sqrt{\frac{1}{N_{\text{lin}}} \sum_{i=1}^{N_{\text{lin}}} (S_i - \bar{S})^2}$ ,  $S_i = \left| \frac{I_{\text{UCL},(i)}}{I_{\text{exp},(i)}} - 1 \right| \cdot 100\%$ ) and the total band strength in cm/molecule. The last column (marked UCL-IAO) contains the data from the present study, the total number of lines in the band, suggested accuracy for the band (in %) and the total band strength in cm/molecule.

Iso.	Band	$N_{\text{lin}}$	Strength	Acc. (%)	$\Delta_{\text{sys}}$ (%)	$\Delta_{\text{stat}}$ (%)	$N_{\text{tot}}$	Strength	Acc. (%)
727	30012-00001	Karlovetz et al. [40] 64	$2.13 \times 10^{-22}$	3-20	+17	13	UCL-IAO 64	$2.22 \times 10^{-22}$	1
	30013-00001	58	$3.48 \times 10^{-22}$	3-20	+13	12		$3.71 \times 10^{-22}$	1
727	30012-00001	Jacquemart et al. [15] 85	$6.85 \times 10^{-23}$	20	+11	2	85	$7.59 \times 10^{-23}$	1
	30013-00001	93	$1.37 \times 10^{-22}$	20	+9	2		$1.50 \times 10^{-22}$	1
	31113-01101	130	$8.84 \times 10^{-24}$	>20	+17	15		$9.21 \times 10^{-24}$	3
828	30012-00001	Karlovetz et al. [40] 64	$1.86 \times 10^{-22}$	10	-2	2	64	$1.83 \times 10^{-22}$	1
	30013-00001	81	$6.05 \times 10^{-22}$	10	-2	3		$6.16 \times 10^{-22}$	1
	00031-00001	80	$1.33 \times 10^{-21}$	10	-13	5		$1.13 \times 10^{-21}$	20
636	30012-00001	Devi et al. [11] 55	$5.41 \times 10^{-24}$	10	+4	3	55	$5.67 \times 10^{-24}$	1
	30013-00001	47	$2.03 \times 10^{-24}$	10	+8	15		$2.18 \times 10^{-24}$	1

requirements.

In order to relate results from the present study to data given in HITRAN we compared line intensities for matched lines between the two line lists (see Table 1). As a primary measure of relative intensity deviation from HITRAN data we used the following formula:

$$S = \left( \frac{I_{\text{UCL}}}{I_{\text{HIT}}} - 1 \right) \cdot 100\% \quad (1)$$

where  $I_{\text{UCL}}$  stands for line intensity from UCL-IAO line list given in cm/molecule and  $I_{\text{HIT}}$  is HITRAN2012 intensity.

This measure is adequate for small deviations but poorly illustrates highly discrepant intensities, due to its asymmetric functional form. For larger deviations, especially for line intensities weaker than HITRAN by more than 100%, the quasi-symmetry is noticeably broken, resulting in a biased picture. In such cases, for example to show graphically a general overview, we decided to use a symmetrized measure to account for proper representation of large deviations:

$$S_{\text{sym}} = \left( \frac{I_{\text{UCL}}}{I_{\text{HIT}}} - \frac{I_{\text{HIT}}}{I_{\text{UCL}}} \right) \cdot 100\% \quad (2)$$

This measure, in turn, yields far from intuitive numbers near 0% deviation.

### 3.8.1. Isotopologue 636

The HITRAN2012 line list for the second most abundant 636 isotopologue contains 68 856 lines below  $8000 \text{ cm}^{-1}$ . There are two sources of line intensities: the majority of lines taken from the 2008 version of the CDSD-296 database [9] and two bands (20012-00001 and 20013-00001) from high precision measurements by Toth et al. [50]. All lines present in the HITRAN2012 database for this isotopologue were matched to our line list with a root mean squared deviation (RMSD) of  $0.04 \text{ cm}^{-1}$ . Lines that lie far in intensity from our predictions (*vide infra*) were double checked by manual investigation.

An overview from Fig. 12 reveals a rather typical situation of funnel shaped relative deviation plot. By zooming into the region

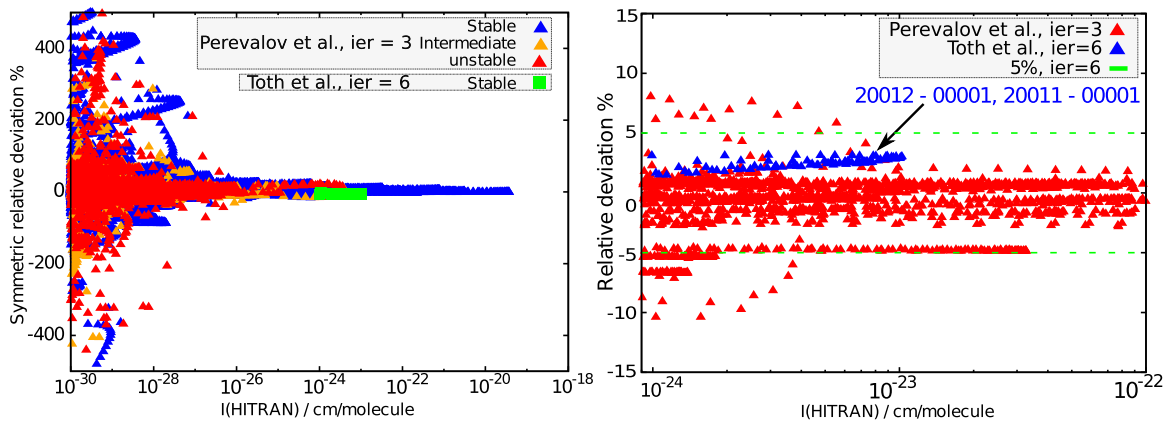


**Fig. 12.** Left panel represents symmetric relative deviation for the 636 isotopologue for the two different sources (Perevalov et al. [9] and Toth et al. [50]) from the HITRAN2012 database. Right panel is a zoomed image in the region of high accuracy (*ier*=6) measurement by Toth et al. Dashed green line indicates 5% limit of deviation tolerance associated with *ier*=6. Two bands measured by Toth et al. are marked with an arrow. (For interpretation of the references to color in this figure caption, the reader is referred to the web version of this paper.)

of high accuracy measurement by Toth et al., one can clearly see that all lines (marked with blue filled triangles in the right panel of Fig. 12) remain within the claimed 5% uncertainty, additionally exhibiting a very narrow spread.

### 3.8.2. Isotopologue 727

HITRAN2012 line list for the 727 isotopologue contains 5187 lines below  $8000\text{ cm}^{-1}$ , all of which were taken from the effective Hamiltonian calculations by Tashkun and Perevalov [51]. Fig. 13 compares our line intensities (all stable) to HITRAN2012; we observe the majority of line intensities display a systematic shift of  $-6\%$  with respect to those recommended by HITRAN. Here again, noticeable arc structures appear. Similar behavior was observed for the main 626 isotopologue. Although most of the arcs are rather flat, there are a few bands which arc structure extends over a wide deviation range. Such occurrences may be caused by insufficiently flexible functional form of the Herman–Wallis factors employed to reduce experimental data for those bands, resulting in inaccurately retrieved experimental line intensities, especially for high  $J$ 's. These serve as an input to the effective Hamiltonian calculations (CDS, hence HITRAN), thus artifacts of experimental analysis are likely to be propagated within the EH approach.

We have already shown that inaccuracies of our model are largely reflected in systematic shifts of whole bands, rather than statistical scatter, which is assumed to remain almost constant as a function of  $J$ . Two bands in Fig. 13 lie outside the tolerance given by the HITRAN2012 uncertainty code 3. These are the 00031–00001 band and the 30013–00001 band (both indicated with arrows in Fig. 13). The discrepancy for the former band has been explained in terms of rather poor reproduction of the  $3\nu_3$  series of bands by our DMS and needs to be replaced in our recommended line list. The behavior of the latter band however is not clearly understood at this stage and requires further investigation. Our working hypothesis is that the  $-6\%$  systematic shift applies to all bands, hence the 30013–00001 band when shifted by  $+6\%$ , should match the 20% tolerance region, which is also regarded as provisional. New measurements by Karlovets et al. [5] and Jacquemart et al. [15] analyzed in the previous section improved the quality of the line positions and intensities for the 30013–00001 band.

### 3.8.3. Isotopologue 828

HITRAN2012 line list for the 828 isotopologue contains 7071 lines below  $8000\text{ cm}^{-1}$ . There are three sources of line intensities: 6280 lines taken from CDS-296 [9] with  $ier$  equal to 3 and 4722 lines taken from a 1994 update to older variational calculations [52] with  $ier$  equal to 2, and finally 69 lines taken from

measurements by Toth et al. [50] with  $ier$  assigned to 3. Fig. 14 compares intensities from the present study to HITRAN2012 data. Despite the low uncertainty index, line intensities originating from Rothman et al. [52] agree within  $\pm 20\%$  with our results. Transitions around  $2.06\text{ }\mu\text{m}$  measured by Toth et al. [50] are enclosed in 10% region reflecting the  $ier$  value for this set. Data points originating from CDS-296 are divided into two sets with differing uncertainty index. The more accurate subset (marked with orange rotated crosses) is clearly squeezed along the relative deviation axis and exhibits almost no systematic shift. In contrast, the lower accuracy subset from CDS spreads over a large region in relative deviation space. This suggests that both sets were calculated with separate input parameters of different qualities. The 30013–00001 band ( $ier=4$ ) deviates around  $+2\%$  from CDS predictions, while the relatively strong 00031–00001 band ( $ier=4$ ) lies 11% below the zero deviation line (visible in Fig. 14). It should be noted that large deviations of the lower accuracy CDS-296 data ( $ier=3$ ) occur for very weak lines, for each the respective experimental data to fit the effective dipole moment parameters are absent. In these cases the parameters of the principal isotopologue were used in CDS-296.

Fig. 15 shows that all strong lines ( $>10^{-28}\text{ cm/molecule}$ ) follow funnel shape envelope, thereby reflecting the typical relation between intensity and accuracy of lines. However several weaker lines, which constitute whole bands, align in wide arc structures with large systematic shift. This is particularly visible for lowered accuracy lines from HITRAN2012 (blue crosses in Fig. 15). These lines were directly incorporated from HITRAN2008. The current release of the CDS database improved on accuracy of these weak lines. A comparison between UCL and CDS-296 intensities is given in Fig. 16.

### 3.8.4. Isotopologue 838

Only limited data are available for the 838 isotopologue in the 2012 edition of HITRAN. 121 lines measured by Toth et al. [50] have uncertainty flag 3 and cover three bands in the  $2\text{ }\mu\text{m}$  region: 20011–00001, 20012–00001 and 20013–00000. All lines present in this set are matched to our line list with a  $\text{RMSD} = 0.04\text{ cm}^{-1}$ . Here, similar to the 727 case, a systematic shift of around 10% is visible. This causes three transitions to breach the stipulated accuracy tolerance. Nevertheless, this should be considered as rather illusory due to the systematic shift of lines coming from all three

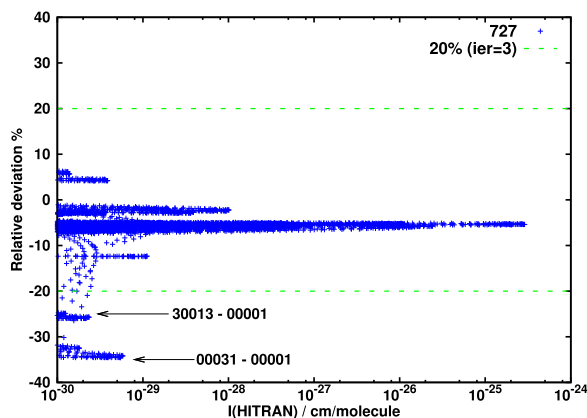


**Fig. 13.** Relative intensities (cf. Eq. (2)) plotted against HITRAN2012 line intensities for the 727 isotopologue. Green dashed horizontal line represents deviation from HITRAN2012 data equal to  $\pm 20\%$ . (For interpretation of the references to color in this figure caption, the reader is referred to the web version of this paper.)

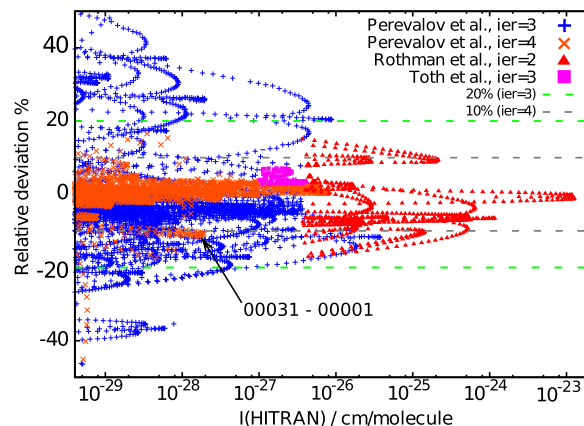


**Fig. 14.** Relative intensities from the present study plotted against HITRAN2012 line intensities for the 828 isotopologue. Only  $\pm 50\%$  region is depicted. Dashed gray and green lines correspond to 10% and 20% deviation, respectively. Blue crosses correspond to a subset of lines taken from Perevalov et al. [9] which has been assigned to  $ier=4$ . Consequently, rotated orange crosses represent  $ier=3$  from the same reference. Red filled triangles refer to Rothman et al. [52], while purple filled squares stand for the small set of lines provided by Toth et al. [50]. (For interpretation of the references to color in this figure caption, the reader is referred to the web version of this paper.)

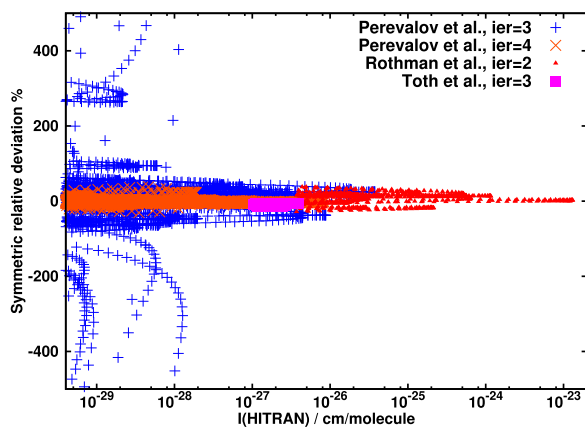


**Fig. 15.** Symmetric relative intensities (cf. Eq. (2)) plotted against HITRAN2012 line intensities for the 828 isotopologue. Only the  $\pm 500\%$  region is depicted. Blue crosses correspond to a subset of lines taken from Perevalov et al. [9] which has been assigned to  $ier=4$ . Consequently, rotated orange crosses represent  $ier=3$  from the same reference. Red filled triangles refer to Rothman et al. [52], while purple filled squares stand for the small set of lines provided by Toth et al. [50]. (For interpretation of the references to color in this figure caption, the reader is referred to the web version of this paper.)

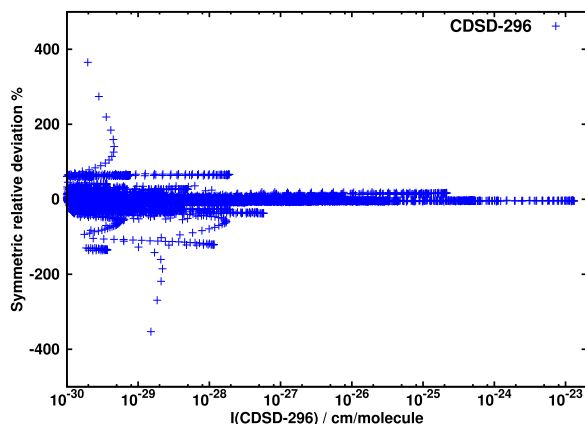


**Fig. 16.** Symmetric relative intensities (cf. Eq. (2)) plotted against CDSD-296 line intensities for the 828 isotopologue. Only the  $\pm 500\%$  region is depicted.

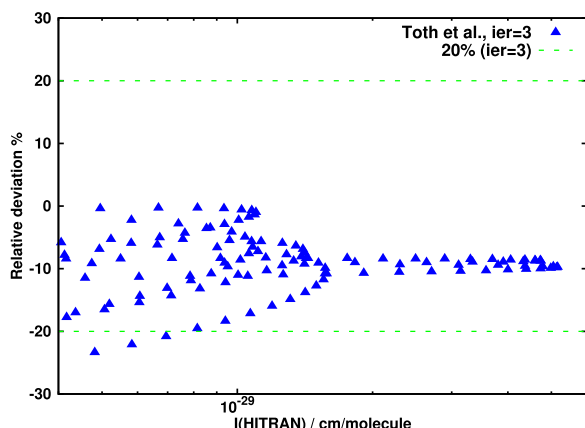


**Fig. 17.** Relative intensities plotted against HITRAN2012 line intensities for the 838 isotopologue. The triangles represent the 121 lines measured by Toth et al. [50] and included in the current version of HITRAN.

bands. Fig. 17 shows calculated intensities relative to HITRAN2012, where all computed lines are classified as stable.

### 3.8.5. Overview

A natural question to ask is if the accuracy of our computational

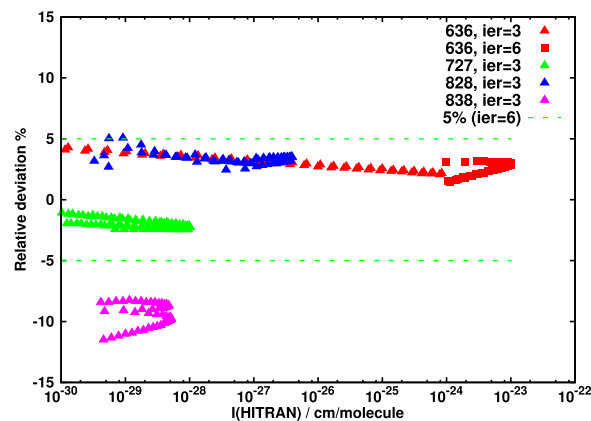


**Fig. 18.** Relative intensities plotted against HITRAN2012 line intensities for the 20012–00001 band for four symmetric isotopologues. Red filled squares represent lines (636) measured by Toth et al. [50] appearing with  $ier=6$ . The remaining lines have code  $ier=3$ . (For interpretation of the references to color in this figure caption, the reader is referred to the web version of this paper.)

scheme based on *ab initio* DMS holds at the same level for all symmetric isotopologues. The current status of experimental accuracy does not give a definite answer to this question and there is a clear need for high accuracy measurements. In the meantime we formulate a weaker query: Do line intensities for a chosen band maintain similar relative deviation from consistent, highly accurate experimental data source for all symmetric isotopologues? Unfortunately, HITRAN2012 contains no such band. Arguably the most important band from an astrophysical and atmospheric measurements perspective is the 20012–00001 band, located in the 2  $\mu\text{m}$  wavelength region. A comparative study for this band for different  $\text{CO}_2$  symmetric isotopologues is therefore given below in Fig. 18.

It is instructive to follow changes in relative intensity deviation among different isotopologues for the selected band. Two data sources were used for this band: a small set of low  $J$  lines from experiment by Toth et al. [50] for the 636 isotopologue (given uncertainty index 6) and CDSD-296 for rest of the lines ( $ier=3$ ). All lines compared above match the stipulated HITRAN uncertainty, that is lines with  $ier=6$  fit the 5% tolerance, and the rest of the lines are 20% or less away from HITRAN2012 values. Minor discontinuity related to change of source of data is seen for the 636 isotopologue. We conclude that the results illustrated in Fig. 18 give a tentative validation of the consistency of our approach with the analyzed database. Relatively good overall agreement between our line list and HITRAN2012, revealing only sporadic deviations that exceed the claimed HITRAN accuracy, but yet justified and facilitated with comparisons with recent and highly accurate measurements, allow us to draw a conclusion that replacing current HITRAN line intensities with our computed values would significantly increase the accuracy, reliability and consistency of the database.

### 3.8.6. Ames-1

In Table 3 we present comparison of root-mean-square-residuals of intensities between Ames-1 DMS, UCL DMS and CDSD-296 for 14 strongest bands of  $\text{CO}_2$  for six symmetric isotopologues. By looking at a given isotopologue, a general trend is that the perpendicular bands ( $\Delta l = +1, +2, \dots$ ) are in worse agreement with CDSD than the parallel bands. On average, UCL-IAO based band intensities are in better agreement with CDSD than Ames for 626 and 636. The 828 isotopologue exhibits a similar level of agreement, and larger deviations for UCL-IAO bands are observed for 727, 838 and 737. This may have two causes: (a) the UCL treatment does not include any beyond Born–Oppenheimer

**Table 3**  
DMS statistics for 14 strongest carbon dioxide bands for six symmetric isotopologues. Numbers in columns correspond to root-mean-square-deviations of band intensities from the CDS-296 database.

Isotopologue Band	Stability	626 UCL-IAO	Ames	636 UCL-IAO	Ames	828 UCL-IAO	Ames	727 UCL-IAO	Ames	838 UCL-IAO	Ames	737 UCL-IAO	Ames
00011–00001	Stable	0.2	2.1	0.8	2.5	1.9	0.5	4.6	2.3	5.7	3.4	4.9	1.8
01101–00001	Stable	1.9	1.7	2.9	2.6	2.3	2.4	5.9	1.4	4.9	4.7	5.0	4.0
01111–01101	Stable	0.2	2.2	0.7	2.5	1.8	0.8	4.6	2.2	5.6	3.7	4.9	1.7
02201–01101	Stable	2.2	2.1	7.3	7.0	2.7	2.5	6.3	1.6	5.4	5.0	5.3	4.2
02211–02201	Stable	0.2	2.2	0.7	2.6	1.8	0.6	4.5	2.3	5.7	3.3	4.9	1.7
03301–01101	Stable	2.5	2.2	11.2	10.9	3.1	2.9	6.6	2.0	5.8	5.5	–	–
10001–01101	Stable	2.0	1.7	0.5	0.9	2.5	2.2	6.1	1.2	5.0	4.3	4.9	3.4
10002–01101	Stable	1.7	1.9	1.9	2.1	2.4	2.5	5.9	1.5	5.3	5.3	5.2	4.3
10011–00001	Stable	0.7	0.8	4.3	4.1	6.9	7.1	4.9	9.4	3.1	3.0	4.7	3.7
10011–10001	Stable	0.3	2.1	0.7	2.7	1.9	0.5	4.6	2.2	5.7	3.3	4.9	1.7
10012–00001	Stable	1.6	1.9	1.6	1.6	8.3	9.1	5.4	10.4	3.5	2.8	6.4	4.8
10012–10002	Stable	0.3	2.1	0.7	2.6	1.9	0.5	4.6	2.2	5.7	3.3	4.8	1.7
11111–01101	Stable	0.9	0.9	4.4	4.3	3.6	3.6	5.0	9.4	2.3	2.3	3.8	2.9
11112–01101	Stable	2.1	2.5	2.4	3.0	3.6	4.5	5.2	10.3	3.2	2.4	6.3	4.6

correction, which may be a source of errors for other than main isotopologue, against which the DMS was benchmarked; (b) CDS entries, as experimentally tuned, are less accurate for less abundant isotopologues, and derived uncertainties do not allow us to judge in favor of either DMS. On balance we believe the second explanation is more likely.

### 3.9. Radioactive isotopologue

Due to its trace atmospheric abundance,  $1.234(14) \times 10^{-12}$  fractional abundance [20], only the strongest ro-vibrational absorption lines of radiocarbon dioxide ( $^{14}\text{C}^{16}\text{O}_2$ , 646) are accessible to accurate measurements. There are only 36 lines (all belonging to the 00011–00001 band) which have intensities above  $10^{-30}$  cm/molecule at room temperature, of which only  $P(20)$  line ( $2209.10 \text{ cm}^{-1}$ ) is located in a spectral region free of major interferences from other abundant atmospheric species like  $\text{H}_2\text{O}$  or  $\text{CH}_4$ . For this reason, this line is most commonly chosen as a reference for determination of radioactive carbon concentrations. Therefore, the  $P(20)$  line of the asymmetric stretching fundamental plays a distinct role in monitoring of carbon dioxide emission caused by fossil fuel combustion.

Although knowledge of the absolute value of the line strength to obtain the  $^{14}\text{C}$  concentrations in SCAR measurements performed on fossil samples [4] can be avoided by using a more convoluted experimental procedure, encouraged by a successful retrieval of natural abundance of 646 by utilizing theoretically calculated line intensity (claimed 5% accurate) by Galli et al. [24], we hope that our updated and plausibly sub-percent accurate intensities will be utilized in future experiments as a reference or calibration data. Usually, a sample to be analyzed is cooled down to 195 K or 170 K in order to diminish interference effects from the nearby (separated by 230 MHz) line of the 636 isotopologue ( $P(19)$  line of the 05511–05501 band). For this reason attention is also paid to line intensities at low temperature for this particular transition. Table 4 compares intensities of the  $P(20)$  and  $P(40)$  lines obtained from several measurements and theoretical calculations together with their respective uncertainties.

Both  $P(20)$  and  $P(40)$  lines are considered stable according to our sensitivity analysis ( $\rho = 1.026$ ). Line intensity given by Galli et al. agrees to 1% with our value for  $T = 195 \text{ K}$ . Genoud et al. give room temperature line intensity flagged with 10% uncertainty, which lies 11% below our prediction. The  $P(20)$  line is 5 times stronger than  $P(40)$ , however the latter one is located in a less crowded spectral region. From this reason McCartt et al. used the  $P(40)$  line to produce calibration curve for concentration of radioactive carbon in the SCAR technique, where reference

**Table 4**  
Intensities of the  $P(20)$  and  $P(40)$  lines of the 00011–00001 band for  $^{14}\text{CO}_2$  taken from different experimental sources.

Reference	Temperature (K)	Strength(uncertainty) $\times 10^{-18}$ cm/molecule
$P(20)$ Galli et al. [24]	195	3.10(15)
$P(20)$ Present study	195	3.07(3)
$P(20)$ Genoud et al. [6]	295	2.52(26)
$P(20)$ Present study	295	2.82(3)
$P(20)$ Present study	170	2.97(3)
$P(40)$ McCartt et al. [26]	300	0.627(30)
$P(40)$ Present study	300	0.572(6)

concentrations were determined by accelerator mass spectrometry. In their spectroscopic model, McCartt et al. use a line intensity at 300 K taken from measurements by Galli et al. [24] (9% above the UCL-IAO intensity) and line intensities of interfering isotopologues from the HITRAN2012 database. This leads to negative concentrations resulting from fitted calibration curve. One of the possible reasons for that could be inaccurate line strength used in the retrieval model. Of equal importance are however: the accuracy of  $^{14}\text{C}$  abundance in samples and the intensities of the satellite lines of other carbon dioxide isotopologues. Here we provide line intensities which are internally consistent and proved to agree within experimental uncertainty to state-of-the-art measurements. Table 4 also lists our prediction for the line intensity at  $T = 170 \text{ K}$ , a temperature which is commonly used for intensity measurements for the  $P(20)$  line.

Vibrational assignments of the UCL line list for 646 were based on isotopic shifts of energy levels and respective assignments for the 626 and 636 isotopologues. After that a comparison of the DVR3D line positions to experimental frequencies by Dobos et al. [53] was made. The tunable diode laser measurements supplied accuracy of  $0.001 \text{ cm}^{-1}$  or better in the  $2229\text{--}2259 \text{ cm}^{-1}$  spectral range of the asymmetric stretching fundamental; this yields an RMSD =  $0.004 \text{ cm}^{-1}$ . This result shows that calculated line positions deviate from experiment just above the stated experimental accuracy, hence may be considered as highly reliable for the 00011–00001 band. For this band the average deviation from the EH calculations for 5 symmetric isotopologue levels is  $0.018 \text{ cm}^{-1}$ , which could probably be reduced by treatment of mass-dependent non-Born–Oppenheimer effects. A more recent study performed by Galli et al. [7], where high-resolution optical-frequency-comb-assisted cavity ring-down technique was used to measure ro-vibrational line positions in  $2190\text{--}2250 \text{ cm}^{-1}$  region with accuracy



of few MHz. Comparison with this study resulted in  $0.005\text{ cm}^{-1}$  RMSD, thereby establishing the provisional uncertainty of the DVR3D line positions to  $0.005\text{ cm}^{-1}$  for the asymmetric stretching fundamental. The study by Galli et al. awaits accurate intensity evaluation. This creates an opportunity for further utilization of our results and comparison with experiments, when done.

The  $3\nu_3$  family of bands discussed in Ref. [3] and in the preceding sections of this article has been proven to be on average 12% too weak in present calculations. For isotopologues other than the radioactive  $^{14}\text{C}^{16}\text{O}_2$  intensities for these bands were replaced with CDS-296 entries. For  $^{14}\text{C}^{16}\text{O}_2$  these intensities were scaled by 1.12 to correct for the systematic differences known from other isotopologues.

### 3.10. Recommended line lists

For all six isotopologues two types of line lists were prepared. First, files named 'UCL-296-isotopologue\_name.dat' contain line positions calculated using Ames-1 PES with DVR3D program and line intensities using UCL DMS. Each line is supplemented with the appropriate scatter factor, given in the last column (see supplementary materials). Vibrational assignments are taken from the newest version of the CDS-296 database. The second set of line lists, called 'recommended UCL-IAO line list' borrows line positions from the effective Hamiltonian calculations (see Section 2.3) whenever a match was possible between Ames-1 PES based line positions from UCL and the effective Hamiltonian values. In rare cases when such match could not be found, line positions were transferred from the CDS-296 database. The scheme used for the line intensities is similar to the one used for the main isotopologue. The  $3\nu_3$  bands and unstable lines were taken from the effective Hamiltonian calculations, and appropriate uncertainty indices were assigned. Intensities of stable lines belonging to bands stronger than  $10^{-23}\text{ cm/molecule}$  (for unit abundance) were taken from UCL DMS calculations and assigned HITRAN uncertainty code 8 (i.e. accuracy of 1% or better). Stable lines belonging to parallel bands weaker than  $10^{-23}\text{ cm/molecule}$  also come from UCL DMS computation and were given uncertainty code 7 (i.e. accuracy 1–2%). Intermediate lines and stable lines belonging to perpendicular bands weaker than  $10^{-23}\text{ cm/molecule}$  feature HITRAN uncertainty code 6 (i.e. accuracy 2–5%). All line positions and line intensities for which scatter factor was not assigned were taken from CDS-296. This was the case for only 3700 weak lines in total for all isotopologues. Both types of line lists are given in the supplementary materials with appropriate explanation in text files. Abundances were taken from the HITRAN2012 database with intensity cut-off  $10^{-30}\text{ cm/molecule}$ . For the radiocarbon isotopologue unit abundance was assumed and  $10^{-27}\text{ cm/molecule}$  intensity cut-off  $\text{cm/molecule}$ .

## 4. Conclusion

In the present study we compute new line lists for six symmetric isotopologues of carbon dioxide:  $^{13}\text{C}^{16}\text{O}_2$ ,  $^{14}\text{C}^{16}\text{O}_2$ ,  $^{12}\text{C}^{17}\text{O}_2$ ,  $^{12}\text{C}^{18}\text{O}_2$ ,  $^{13}\text{C}^{17}\text{O}_2$  and  $^{13}\text{C}^{18}\text{O}_2$ . Detailed comparisons with both the theoretical and experimental works indicate the high accuracy of the line intensities resulting from our *ab initio* DMS. Sensitivity analysis of the line intensities performed here confirmed the existence of several resonance interactions already reported in the literature, altogether with predictions for new pairs of energy levels involved in strong interactions. We hope that the methodology presented and evaluated here will be of use in theoretical approaches to other molecules. Accurate line positions generated using an effective Hamiltonian combined with highly accurate line intensities give comprehensive line lists, which we recommend for

use in remote sensing studies and inclusions in databases.

This paper completes our analysis of the transition intensities of symmetric isotopologues of  $\text{CO}_2$ . We are currently analyzing the transition intensities of the asymmetric isotopologues. This work raises some theoretical issues as the loss of symmetry has consequences for both the DVR3D nuclear motion calculations and the CDS effective Hamiltonian studies. Results will be reported in the near future [54].

## Acknowledgments

This work is supported by the UK Natural Environment Research Council (NERC) through grant NE/J010316, the ERC under the Advanced Investigator Project 267219 and the Russian Fund for Fundamental Studies. The authors acknowledge the use of the UCL Legion High Performance Computing Facility (Legion@UCL), and associated support services, in the completion of this work.

## Appendix A. Supplementary data

Supplementary data associated with this article can be found in the online version at <http://dx.doi.org/10.1016/j.jqsrt.2016.11.022>.

## References

- [1] Miller CE, Crisp D, DeCola PL, Olsen SC, Randerson JT, Michalak AM, et al. Precision requirements for space-based X-CO<sub>2</sub> data. *J Geophys Res* 2007;112: D10314. <http://dx.doi.org/10.1029/2006JD007659>.
- [2] Polyansky OL, Bielska K, Ghyssels M, Lodi L, Zobov NF, Hodges JT, et al. High accuracy CO<sub>2</sub> line intensities determined from theory and experiment. *Phys Rev Lett* 2015;114:243001. <http://dx.doi.org/10.1103/PhysRevLett.114.243001>.
- [3] Zak E, Tennyson J, Polyansky OL, Lodi L, Tashkun SA, Perevalov VI. A room temperature CO<sub>2</sub> line list with *ab initio* computed intensities. *J Quant Spectrosc Radiat Transf* 2016;177:31–42. <http://dx.doi.org/10.1016/j.jqsrt.2015.12.022>.
- [4] Galli I, Bartalini S, Cancio P, De Natale P, Mazzotti D, Giusfredi G, et al. Optical detection of radiocarbon dioxide: first results and AMS intercomparison. *Radiocarbon* 2013;55:213–223.
- [5] Karlovets EV, Campargue A, Mondelain D, Kass S, Tashkun SA, Perevalov VI. High sensitivity Cavity Ring Down spectroscopy of <sup>18</sup>O enriched carbon dioxide between 5850 and 7000  $\text{cm}^{-1}$ : Part III Analysis and theoretical modeling of the <sup>12</sup>C<sup>17</sup>O<sub>2</sub>, <sup>16</sup>O<sup>12</sup>C<sup>17</sup>O, <sup>17</sup>O<sup>12</sup>C<sup>18</sup>O, <sup>16</sup>O<sup>13</sup>C<sup>17</sup>O and <sup>17</sup>O<sup>13</sup>C<sup>18</sup>O spectra. *J Quant Spectrosc Radiat Transf* 2014;136:89–107. <http://dx.doi.org/10.1016/j.jqsrt.2013.11.006>.
- [6] Genoud G, Vainio M, Phillips H, Dean J, Merimaa M. Radiocarbon dioxide detection based on cavity ring-down spectroscopy and a quantum cascade laser. *Opt Lett* 2015;40:1342. <http://dx.doi.org/10.1364/ol.40.001342>.
- [7] Galli I, Pastor PC, Di Leonardo G, Fusina L, Giusfredi G, Mazzotti D, et al. The  $\nu_3$  band of <sup>14</sup>C<sup>16</sup>O<sub>2</sub> molecule measured by optical-frequency-comb-assisted cavity ring-down spectroscopy. *Mol Phys* 2011;109:2267–2272. <http://dx.doi.org/10.1080/00268976.2011.614284>.
- [8] Rothman LS, Gordon IE, Babikov Y, Barbe A, Benner DC, Bernath PF, et al. The HITRAN 2012 molecular spectroscopic database. *J Quant Spectrosc Radiat Transf* 2013;130:4–50. <http://dx.doi.org/10.1016/j.jqsrt.2013.07.002>.
- [9] Perevalov VI, Tashkun SA. CDS-296 (Carbon Dioxide Spectroscopic Databank): updated and enlarged version for atmospheric applications. Cambridge MA, USA, 2008.
- [10] Tashkun SA, Perevalov VI, Gamache RR, Lamouroux J. CDS-296, high resolution carbon dioxide spectroscopic databank: Version for atmospheric applications. *J Quant Spectrosc Radiat Transf* 2015;152:45–73. <http://dx.doi.org/10.1016/j.jqsrt.2014.10.017>.
- [11] Devi VM, Benner DC, Sung K, Brown LR, Crawford TJ, Miller CE, et al. Line parameters including temperature dependences of self- and air-broadened line shapes of <sup>12</sup>C<sup>16</sup>O<sub>2</sub>: 1.6-  $\mu\text{m}$  region. *J Quant Spectrosc Radiat Transf* 2016;177:117–144. <http://dx.doi.org/10.1016/j.jqsrt.2015.12.020>.
- [12] Jacquemart D, Gueye F, Lyulin OM, Karlovets EV, Baron D, Perevalov VI. Infrared spectroscopy of CO<sub>2</sub> isotopologues from 2200 to 7000  $\text{cm}^{-1}$ : I—characterizing experimental uncertainties of positions and intensities. *J Quant Spectrosc Radiat Transf* 2012;113:961–975. <http://dx.doi.org/10.1016/j.jqsrt.2012.02.020>.
- [13] Borkov YG, Jacquemart D, Lyulin OM, Tashkun SA, Perevalov VI. Infrared spectroscopy of <sup>17</sup>O- and <sup>18</sup>O-enriched carbon dioxide: line positions and intensities in the 3200–4700  $\text{cm}^{-1}$  region. Global modeling of the line positions of <sup>16</sup>O<sup>12</sup>C<sup>17</sup>O<sub>2</sub> and <sup>17</sup>O<sup>12</sup>C<sup>17</sup>O. *J Quant Spectrosc Radiat Transf* 2014;137:57–76. <http://dx.doi.org/10.1016/j.jqsrt.2013.11.008>.

- [14] Borkov YG, Jacquemart D, Lyulin OM, Tashkun SA, Perevalov VI. Infrared spectroscopy of  $^{17}\text{O}$ - and  $^{18}\text{O}$ -enriched carbon dioxide: line positions and intensities in the 4681–5337  $\text{cm}^{-1}$  region. *J Quant Spectrosc Radiat Transf* 2015;159:1–10. <http://dx.doi.org/10.1016/j.jqsrt.2015.02.019>.
- [15] Jacquemart D, Borkov Y, Lyulin OM, Tashkun SA, Perevalov VI. Fourier transform spectroscopy of  $\text{CO}_2$  isotopologues at 1.6  $\mu\text{m}$ : line positions and intensities. *J Quant Spectrosc Radiat Transf* 2015;160:1–9. <http://dx.doi.org/10.1016/j.jqsrt.2015.03.016>.
- [16] Durry G, Li JS, Vinogradov I, Titov A, Joly L, Cousin J, et al. Near infrared diode laser spectroscopy of  $\text{C}_2\text{H}_2$ ,  $\text{H}_2\text{O}$ ,  $\text{CO}_2$  and their isotopologues and the application to TDLAS, a tunable diode laser spectrometer for the Martian PHOBOS-GRUNT space mission. *Appl Phys B* 2010;99:339–351. <http://dx.doi.org/10.1007/s00340-010-3924-y>.
- [17] Huang X, Schwenke DW, Tashkun SA, Lee TJ. An isotopic-independent highly accurate potential energy surface for  $\text{CO}_2$  isotopologues and an initial  $^{12}\text{C}^{16}\text{O}_2$  infrared line list. *J Chem Phys* 2012;136:124311. <http://dx.doi.org/10.1063/1.3697540>.
- [18] Huang X, Gamache RR, Freedman RS, Schwenke DW, Lee TJ. Reliable infrared line lists for 13  $\text{CO}_2$  isotopologues up to  $E=18,000\text{ cm}^{-1}$  and 1500 K, with line shape parameters. *J Quant Spectrosc Radiat Transf* 2014;147:134–144. <http://dx.doi.org/10.1016/j.jqsrt.2014.05.015>.
- [19] Reick CH, Raddatz T, Pongratz J, Claussen M. Contribution of anthropogenic land cover change emissions to pre-industrial atmospheric  $\text{CO}_2$ . *Tellus B* 2010;62:329–336. <http://dx.doi.org/10.1111/j.1600-0889.2010.00479.x>.
- [20] Levin I, Naegler T, Kromer B, Diehl M, Francey RJ, Gomez-Pelaez AJ, et al. Observations and modelling of the global distribution and long-term trend of atmospheric  $^{14}\text{CO}_2$ . *Tellus B* 2010;62:26–46. <http://dx.doi.org/10.1111/j.1600-0889.2009.00446.x>.
- [21] Rose KA, Sikes EL, Guilderson TP, Shane P, Hill TM, Zahn R, et al. Upper-ocean-to-atmosphere radiocarbon offsets imply fast deglacial carbon dioxide release. *Nature* 2010;466:1093–1097. <http://dx.doi.org/10.1038/nature09288>.
- [22] Tomita H, Watanabe K, Takiguchi Y, Kawarabayashi J, Iguchi T. Radioactive carbon isotope monitoring system based on cavity ring-down laser spectroscopy for decommissioning process of nuclear facilities. *J Power Energy Syst* 2008;2:221–228. <http://dx.doi.org/10.1299/jpes.2.221>.
- [23] Giusfredi G, Galli I, Mazzotti D, Cancio P, De Natale P. Theory of saturated-absorption cavity ring-down: radiocarbon dioxide detection, a case study. *J Opt Soc Am B* 2015;32:2223. <http://dx.doi.org/10.1364/josab.32.002223>.
- [24] Galli I, Bartalini S, Borri S, Cancio P, Mazzotti D, De Natale P, et al. Molecular gas sensing below parts per trillion: Radiocarbon-dioxide optical detection. *Phys Rev Lett* 2011;107:270802. <http://dx.doi.org/10.1103/physrevlett.107.270802>.
- [25] Giusfredi G, Bartalini S, Borri S, Cancio P, Galli I, Mazzotti D, et al. Saturated-absorption cavity ring-down spectroscopy. *Phys Rev Lett* 2010;104:110801. <http://dx.doi.org/10.1103/physrevlett.104.110801>.
- [26] McCart A, Ognibene T, Bench G, Turteltaub K. Measurements of carbon-14 with cavity ring-down spectroscopy. *Nucl Instrum Methods Phys Res Sect B: Beam Interact Mater Atoms* 2015;361:277–280. <http://dx.doi.org/10.1016/j.nimb.2015.05.036>.
- [27] Guimbaud C, Noël C, Chartier M, Catoire V, Blessing M, Gourry JC, et al. A quantum cascade laser infrared spectrometer for  $\text{CO}_2$  stable isotope analysis: field implementation at a hydrocarbon contaminated site under bio-remediation. *J Environ Sci* 2016;40:60–74. <http://dx.doi.org/10.1016/j.jes.2015.11.015>.
- [28] Kireev SV, Shnyrev SL, Kondrashov AA. Development of laser noninvasive on-line diagnostics of oncological diseases based on the absorption method in the 4860–4880  $\text{cm}^{-1}$  spectral range. *Laser Phys* 2016;26:075601. <http://dx.doi.org/10.1088/1054-660X/26/7/075601>.
- [29] Lodi L, Tennyson J. Line lists for  $\text{H}_2^{18}\text{O}$  and  $\text{H}_2^{17}\text{O}$  based on empirically-adjusted line positions and ab initio intensities. *J Quant Spectrosc Radiat Transf* 2012;113:850–858.
- [30] Tennyson J. TRIATOM, SELECT and ROTLEV – for the calculation of ro-vibrational levels of triatomic molecules. *Comput Phys Commun* 1986;42:257–270.
- [31] Sutcliffe BT, Miller S, Tennyson J. An effective computational approach to the calculation of vibration-rotation spectra of triatomic molecules. *Comput Phys Commun* 1988;51:73–82.
- [32] Sutcliffe BT, Tennyson J. A general treatment of vibration-rotation coordinates for triatomic molecules. *Int J Quantum Chem* 1991;39:183–196.
- [33] Tennyson J, Kostin MA, Barletta P, Harris GJ, Polyansky OL, Ramanlal J, et al. DVR3D: a program suite for the calculation of rotation-vibration spectra of triatomic molecules. *Comput Phys Commun* 2004;163:85–116.
- [34] Audi G, Wapstra AH. The 1995 update to the atomic mass evaluation. *Nucl Phys A* 1995;595:409–480. [http://dx.doi.org/10.1016/0375-9474\(95\)00445-9](http://dx.doi.org/10.1016/0375-9474(95)00445-9).
- [35] Huang X, Freedman RS, Tashkun SA, Schwenke DW, Lee TJ. Semi-empirical  $^{12}\text{C}^{16}\text{O}_2$  IR line lists for simulations up to 1500 K and 20,000  $\text{cm}^{-1}$ . *J Quant Spectrosc Radiat Transf* 2013;130:134–146. <http://dx.doi.org/10.1016/j.jqsrt.2013.05.018>.
- [36] Teffo JL, Sulakshina ON, Perevalov VI. Effective Hamiltonian for rovibrational energies and line-intensities of carbon-dioxide. *J Mol Spectrosc* 1992;156:48–64. [http://dx.doi.org/10.1016/0022-2852\(92\)90092-3](http://dx.doi.org/10.1016/0022-2852(92)90092-3).
- [37] Tashkun SA, Perevalov VI, Teffo JL, Rothman LS, Tyuterev V. Global fitting of  $^{12}\text{C}^{16}\text{O}_2$  vibrational-rotational line positions using the effective Hamiltonian approach. *J Quant Spectrosc Radiat Transf* 1998;60:785–801. [http://dx.doi.org/10.1016/S0022-4073\(98\)00082-X](http://dx.doi.org/10.1016/S0022-4073(98)00082-X).
- [38] Tashkun S, Perevalov V, Teffo J-L, Lecoutre M, Huet T, Campargue A, et al.  $^{13}\text{C}^{16}\text{O}_2$ : global treatment of vibrational-rotational spectra and first observation of the  $2v_1 + 5v_3$  and  $v_1 + 2v_2 + 5v_3$  absorption bands. *J Mol Spectrosc* 2000;200:162–176. <http://dx.doi.org/10.1006/jmsp.2000.8057>.
- [39] Tashkun S. Global multi-isotopologue fitting of  $\text{CO}_2$  vibrational-rotational line positions using a phenomenological mass dependent effective Hamiltonian. In: Abstracts of the XVII symposium on high resolution molecular spectroscopy, Zelenogorsk, St.Petersburg Region, Russia, 2012. p. 67.
- [40] Karlovets EV, Campargue A, Mondelain D, Béguier S, Kassi S, Tashkun SA, et al. High sensitivity cavity ring down spectroscopy of  $^{18}\text{O}$  enriched carbon dioxide between 5850 and 7000  $\text{cm}^{-1}$ : I. Analysis and theoretical modeling of the  $^{16}\text{O}^{12}\text{C}^{18}\text{O}$  spectrum. *J Quant Spectrosc Radiat Transf* 2013;130:116–133. <http://dx.doi.org/10.1016/j.jqsrt.2013.05.019>.
- [41] Karlovets E, Campargue A, Mondelain D, Kassi S, Tashkun S, Perevalov V. High sensitivity Cavity Ring Down Spectroscopy of  $^{18}\text{O}$  enriched carbon dioxide between 5850 and 7000  $\text{cm}^{-1}$ : Part II. Analysis and theoretical modeling of the  $^{12}\text{C}^{18}\text{O}_2$ ,  $^{13}\text{C}^{18}\text{O}_2$  and  $^{16}\text{O}^{13}\text{C}^{18}\text{O}$  spectra. *J Quant Spectrosc Radiat Transf* 2014;136:71–88. <http://dx.doi.org/10.1016/j.jqsrt.2013.11.005>.
- [42] Karlovets EV, Perevalov VI. The influence of isotopic substitution on the effective dipole moment parameters of  $\text{CO}_2$  molecule. *Opt Spectrosc* 2015;119:16–21. <http://dx.doi.org/10.1134/s0030400x15070139>.
- [43] Laraia AL, Gamache RR, Lamouroux J, Gordon IE, Rothman LS. Total internal partition sums to support planetary remote sensing. *Icarus* 2011;215:391–400. <http://dx.doi.org/10.1016/j.icarus.2011.06.004>.
- [44] Tashkun SA, Perevalov VI. CDS-4000: high-resolution, high-temperature carbon dioxide spectroscopic databank. *J Quant Spectrosc Radiat Transf* 2011;112:1403–1410. <http://dx.doi.org/10.1016/j.jqsrt.2011.03.005>.
- [45] Benner DC, Devi VM, Sung K, Brown LR, Miller CE, Payne VH, et al. Line parameters including temperature dependences of air- and self-broadened line shapes of  $^{12}\text{C}^{16}\text{O}_2$ : 2.06- $\mu\text{m}$  region. *J Mol Spectrosc* 2016;326:21–47. <http://dx.doi.org/10.1016/j.jms.2016.02.012>.
- [46] Kiseleva M, Mandon J, Persijn S, Petersen J, Nielsen L, Harren FJM. Tractable line strength measurements of methane and carbon dioxide in the near infrared wavelength region at 1.65  $\mu\text{m}$  using cavity ring down spectroscopy. In: 13th ASA-HITRAN conference, Reims, 2016. p. P1–16.
- [47] Rothman LS, Jacquemart D, Barbe A, Benner DC, Birk M, Brown LR, et al. The HITRAN 2004 molecular spectroscopic database. *J Quant Spectrosc Radiat Transf* 2005;96:139–204.
- [48] Rothman LS, Gordon IE, Barbe A, Benner DC, Bernath PF, Birk M, et al. The HITRAN 2008 molecular spectroscopic database. *J Quant Spectrosc Radiat Transf* 2009;110:533–572.
- [49] Toth R, Miller C, Brown L, Devi VM, Benner DC. Line positions and strengths of  $^{16}\text{O}^{12}\text{C}^{18}\text{O}$ ,  $^{18}\text{O}^{12}\text{C}^{18}\text{O}$  and  $^{17}\text{O}^{12}\text{C}^{18}\text{O}$  between 2200 and 7000  $\text{cm}^{-1}$ . *J Mol Spectrosc* 2007;243:43–61. <http://dx.doi.org/10.1016/j.jms.2007.03.005>.
- [50] Toth RA, Brown LR, Miller CE, Devi VM, Benner DC. Spectroscopic database of  $\text{CO}_2$  line parameters: 4300–7000  $\text{cm}^{-1}$ . *J Quant Spectrosc Radiat Transf* 2008;109:906–921. <http://dx.doi.org/10.1016/j.jqsrt.2007.12.004>.
- [51] Tashkun SA, Perevalov VI. Private communication: intensities calculated using the effective dipole moment function; 2012.
- [52] Rothman LS, Hawkins RL, Wattson RB, Gamache RR. Energy levels, intensities, and linewidths of atmospheric carbon dioxide bands. *J Quant Spectrosc Radiat Transf* 1992;48:537–566. [http://dx.doi.org/10.1016/0022-4073\(92\)90119-o](http://dx.doi.org/10.1016/0022-4073(92)90119-o).
- [53] Dobos S, Winnewisser G, Kling F, Mink J. Improved spectroscopic constants for  $^{14}\text{C}^{16}\text{O}_2$  obtained from the  $v_3$  band. *Z Naturforsch* 1989;44a:633–639.
- [54] Zak E, Tennyson J, Polyansky OL, Lodi L, Zobov NF, Tashkun SA, et al. Room temperature line lists for  $\text{CO}_2$  asymmetric isotopologues with ab initio computed intensities. *J Quant Spectrosc Radiat Transf* (2016) submitted for publication.